East African Journal of Biophysical and Computational Sciences
ISSN (Online): 2789-3618 and ISSN (Print): 2789-360X

ARTICLE

ARTICLE INFO
Volume 7(1), 2026
https://dx.doi.org/10.4314/eajbcs.v7i1.1S

ARTICLE HISTORY
Received: 16 November, 2025
Accepted: 30 April, 2026
Published Online: 10 June, 2026

CITATION
Alemu et.al (2026) Bifurcation Analysis of Eco-Epidemiological Mathematical Model with Saturated Incidence Rate and General Holling Type Response Function. *East African Journal of Biophysical and Computational Sciences* Volume 7(1), 2026. .https://dx.doi.org/10.4314/eajbcs.v7i1.1S.1-17

East African Journal of Biophysical and Computational Sciences (EAJBCS) is already indexed on known databases like AJOL, DOAJ, CABI ABSTRACTS and FAO AGRIS.

Bifurcation Analysis of Eco-Epidemiological Mathematical Model with Saturated Incidence Rate and General Holling Type Response Function

Solomon Molla Alemu[1], Tesfaye Tefera Mamo[2], Mohammed Yiha Dawed[3,*]

[1]Addis Ababa Science and Technology University, Department of Mathematics, Addis Ababa, Ethiopia,
[2]Debre Berhan University, Department of Mathematics, Debre Berhan, Ethiopia,
[3]Hawassa University, Department of Mathematics, Hawassa, Ethiopia

*Corresponding author: mohammedyiha@hu.edu.et

Abstract

This paper presents a bifurcation analysis of an Eco-epidemiological model with saturated incidence rate and general Holling-Type functional responses. The model describes a predator–prey system in which the prey population is infected by a communicable disease, and the predator feeds on both susceptible and infected individuals. Fundamental properties of the system, including existence and uniqueness, positivity, and boundedness of solutions, are established to ensure biological feasibility. Equilibrium points are identified and their stability is examined. The basic reproduction number R_0 is derived to determine threshold conditions for disease persistence. Using Sotomayor's theorem, transcritical and Hopf bifurcations are rigorously verified. The results indicate that increasing the inhibition rate stabilizes the system and promotes coexistence, whereas higher transmission rates destabilize equilibria and generate sustained oscillations. Numerical simulations and bifurcation diagrams validate the analytical findings, demonstrating transitions between stable steady states and periodic dynamics.

Keywords: Eco-epidemiology, Saturated incidence rate, Bifurcation, General Holling Type, Emergent carrying capacity

1 Introduction

In applied mathematics, mathematical modeling serves as an essential tool for investigating real-world problems across diverse disciplines, including biology, epidemiology, and ecology (Bezabih et al., 2021). Numerous researchers have demonstrated that the dynamic interactions between predator and prey populations can be effectively analyzed using the tools of mathematical ecology (Das, 2016; Demir, 2019). Building upon the foundational works of Lotka (1925) and Volterra (1927), various sophisticated predator–prey models have been developed to describe complex ecological interactions under different realistic scenarios (Ghanbari, 2021; Sieber et al., 2014). Furthermore, Anderson and May (1986) established a pioneering framework that integrates the epidemiological models of Kermack and McKendrick (Brauer, 2005) with classical Lotka–Volterra predator–prey dynamics. As a result, recent decades have been marked by a growing body of research devoted to analyzing the dynamical behavior of eco-epidemiological models (Biswas et al., 2015). Since conducting experiments is often impractical or unethical, mathematical modeling has become an essential approach for investigating and understanding the transmission and control of infectious diseases. Numerous researchers (e.g., Hugo and Simanjilo (2019) and Sieber et al. (2014)) have explored predator–prey models incorporating disease dynamics, highlighting how infections within the prey and/or predator populations can significantly influence the ecological interactions and system stability. The primary focus of eco-epidemiological models revolves around how infections impact species mortality, decrease reproduction rates, the nature of contamination, changes in population size, the eradication or control of epidemic outbreaks, the persistence and the overarching dynamics of the diseased species (Sieber et al., 2014). Saifuddin et al. (2016) demonstrated that, under an explicit carrying capacity, susceptible and infected prey exhibit identical competitive abilities, whereas under an emergent carrying capacity, infected prey compete less effectively than susceptible ones in the presence of disease. Biswas et al. (2015) examined a modified Lotka-Volterra system that incorporates the prey infection propagation term based on the mass action law, while Haldar et al. (2021) focused on standard incidence within predator-prey interactions. Liu et al. (1987) proposed an epidemiological model characterized by a nonlinear incidence rate. Gumel and Moghadas (2003) formulated

a tritrophic dynamics that incorporating a distinct saturating incidence term to more accurately capture complex transmission dynamics, while Ruan and Wang (2003) extended this line of research by examining an epidemic model that integrates essential system with a saturating incidence term to investigate the overall system behavior. Their approach is deemed more justifiable because it considers behavioral changes and the crowding effect among infected individuals, thus preventing the contact rate from becoming unbounded by selecting appropriate parameters (Maiti et al., 2019). Hu et al. (2017) analyzed a discrete-time eco-epidemiological framework, focusing on the system dynamic behavior under a Holling type-II incidence function in place of the bilinear incidence rate. Following these influential studies have incorporated disease transmission into prey and/or predator populations under various incidence mechanisms, including mass action, standard incidence, and nonlinear forms. Among these, saturated incidence rates have attracted considerable attention because they incorporate behavioral changes and crowding effects, thereby preventing unrealistic unbounded transmission when the infected population becomes large. Such formulations provide a more biologically realistic representation of disease spread.

From an ecological perspective, predator–prey dynamics are strongly influenced by the prey's response to predation, while the predator population, in turn, directly or indirectly regulates the prey population (Panja, 2020). In order to accurately characterize the responsiveness of predation rates to variations in prey biomass across different population densities, ecologically realistic functional responses have been formulated that explicitly incorporate prey behavioral patterns. The following functional responses are developed: Beddington-DeAngelis (Li & Takeuchi, 2011), Crowley-Martin (Maiti et al., 2019), General Holling type (Dawed et al., 2020), Michaelis-Menten type (HT-II), Holling type III, Holling type IV (which came later) (Holling, 1959). Holling responses are commonly categorized into specific forms (Type I–IV), each with distinct ecological characteristics. However, in this study, the use of the term "General Holling-Type functional responses" is intentionally and methodologically justified. We mean either of these forms or combinations of them:

$$f(x) = ax, \quad g(x) = \frac{ax}{b+x}, \quad h(x) = \frac{ax^2}{b+x^2}, \quad r(x) = \frac{ax}{1+bx+cx^2},$$

where, a is attack rate, b is a half saturation constant and c is the measure of the predator tolerance to the prey to attack. Haque and Venturino (2007) studied an eco-epidemic model in which the predator population is infected and predation follows a ratio-dependent functional response. Moreover, Kooi et al. (2011) also have discussed on tritrophics food web eco-epidemiological system with predator infection, where the infection transmitted among predators follow a hybrid response function as Holling type-IV functional response and Beddington–DeAngelis type functional response (Li & Takeuchi, 2011). Capasso and Serio (1978) introduced an interaction term to account for the saturation effect in large infectious populations. Consequently, incorporating saturation in disease transmission (Cai & Li, 2010) becomes particularly relevant in eco-epidemiological models when the number of infectives is high. Real-world predation involves complex mechanisms (Wayesa et al., 2024, 2025) such as prey refuge, handling time, predator interference, and adaptive feeding, which can be captured using general Holling-type functional responses. However, most eco-epidemiological models rely on simplified predation terms and standard disease transmission functions, with limited attention given to combining generalized predation dynamics and saturated incidence. Key research gaps include:

- Lack of systematic analysis of the combined effects of saturated disease transmission and general Holling-type responses on system stability.
- Limited exploration of how these nonlinear mechanisms drive qualitative changes such as transcritical and Hopf bifurcations.
- Few models incorporating emergent carrying capacity with unequal competition between susceptible and infected prey.
- The absence of a rigorous analytical framework linking the basic reproduction number, stability switching, and bifurcation dynamics Wang et al. (2016) under such generalized conditions.

To address these gaps, the study proposes a novel eco-epidemiological model integrating saturated incidence, generalized Holling-type predation on susceptible and infected prey, and an emergent carrying capacity framework with distinct competition effects. This integrated approach strengthens theoretical understanding of system stability, persistence, and complex population oscillations.

The remainder of this paper is organized as follows: Section 2 presents the mathematical formulation of the model; Section 3 establishes fundamental dynamical properties; Section 4 is devoted to stability and bifurcation analysis; Section 5 provides numerical simulations that support the analytical findings; Finally, the concluding section summarizes the main results and discusses their ecological implications.

2 Mathematical Model

In this section, we investigate the eco-epidemiological dynamics to explore the influence of a saturated incidence function on the sustainable coexistence of two interacting species within the same ecosystem. Let $A(t)$ and $B(t)$ denote the prey and predator densities at time t, respectively. The model is formulated based on the following biological assumptions:

The total prey population is divided into two compartments

$$A(t) = A_1(t) + A_2(t)$$

where $A_1(t)$ and $A_2(t)$ represent the susceptible and infected prey populations, respectively.

The researchers assume that the lifespan of infected prey is shorter than that of susceptible prey (Haldar et al., 2021). The susceptible prey population $A_1(t)$ follows logistic growth in the absence of predation and disease. Furthermore, both susceptible and infected prey share limited environmental resources. However, they do not possess identical competitive abilities. To capture this ecological feature, we incorporate distinct competition coefficients representing emergent carrying capacity: b_1 denotes intra-specific competition among susceptible prey, while b_2 represents inter-specific competition between susceptible and infected prey (Ghanbari, 2021; Sieber et al., 2014). Thus, the logistic growth of susceptible prey is given by

$$\frac{dA_1}{dt} = r_{A_1} A_1 \left(1 - b_1 A_1 - b_2 A_2\right).$$

The disease spreads among prey solely through direct contact. Infected prey do not recover or acquire immunity; instead, they are removed from the system through predation, disease-induced mortality at rate δ, and natural death at rate α_1.

We assume that susceptible prey become infected according to a nonlinear saturated incidence function

$$\frac{\beta A_1 A_2}{1 + sA_2}$$

as proposed in Maiti et al. (2019). Here, βA_2 represents the force of infection rate, while $\frac{1}{1+sA_2}$ accounts for behavioral changes and crowding effects among infected individuals. This formulation prevents the transmission rate from becoming unbounded for large infected populations (Ruan & Wang, 2003).

Ecologically, infected prey is generally more vulnerable to predation due to its weakened physiological condition. To capture this phenomenon, we incorporate distinct general Holling-Type functional responses, $\Phi_{A_1}(A_1)$ and $\Phi_{A_2}(A_2)$, which represent the predator's consumption of susceptible and infected prey biomass, respectively.

Accordingly, the susceptible prey dynamics are given by

$$\frac{dA_1}{dt} = r_{A_1} A_1 \left(1 - b_1 A_1 - b_2 A_2\right) - \frac{\beta A_1 A_2}{1 + sA_2} - \Phi_{A_1}(A_1) B,$$

while the infected prey dynamics are described by

$$\frac{dA_2}{dt} = \frac{\beta A_1 A_2}{1+sA_2} - (\alpha_1+\delta)A_2 - \Phi_{A_2}(A_2)B.$$

The model assumes a specialist predator population $B(t)$ that feeds on both susceptible and infected prey, with predation governed by general Holling-type functional responses. Accordingly, the predator's population dynamics are formulated based on these generalized predation interactions.

$$\frac{dB}{dt} = C_1\Phi_{A_1}(A_1)B + C_2\Phi_{A_2}(A_2)B - \alpha_2 B,$$

where C_1 and C_2 denote the conversion efficiencies of susceptible and infected prey into predator biomass, respectively, and α_2 represents the natural mortality rate of the predator.

The descriptions of state variables and parameters are provided in Table 1. All parameters are assumed to be positive. Hence, based on the above assumptions, the governing eco-epidemiological model takes the form

$$\begin{cases} \dfrac{dA_1}{dt} = r_{A_1}A_1\Big(1-b_1A_1-b_2A_2\Big) - \dfrac{\beta A_1A_2}{1+sA_2} - \Phi_{A_1}(A_1)B, \\ \dfrac{dA_2}{dt} = \dfrac{\beta A_1A_2}{1+sA_2} - (\alpha_1+\delta)A_2 - \Phi_{A_2}(A_2)B, \\ \dfrac{dB}{dt} = C_1\Phi_{A_1}(A_1)B + C_2\Phi_{A_2}(A_2)B - \alpha_2 B, \end{cases} \tag{1}$$

with initial conditions

$$A_1(0) = A_1^0 > 0, \quad A_2(0) = A_2^0 \geq 0, \quad B(0) = B^0 > 0. \tag{2}$$

2.1 Non-Dimensionalization

Non-Dimensionalization simplify and make the equations easier to interpret. The transformation equations could be:
$A_1 = \frac{1}{b_1}S, A_2 = \frac{1}{b_1}I, B = \frac{s}{b_1}P, t = \frac{1}{r_{A_1}}T, \Phi_{A_1}$
$(A_1) = \frac{r_{A_1}}{C_1}\psi_S(S)$, and $\Phi_{A_2}(A_2) = \frac{r_{A_1}}{C_2}\psi_I(I)$.

Thus, the scaled form of the dynamical system is

$$\begin{cases} \dfrac{dS}{dT} = S\Big(1-S-\kappa I\Big) - \dfrac{\gamma SI}{1+\eta I} - \theta_1\psi_S(S)P, \\ \dfrac{dI}{dT} = \dfrac{\gamma SI}{1+\eta I} - \zeta I - \theta_2\psi_I(I)P, \\ \dfrac{dP}{dT} = \psi_S(S)P + \psi_I(I)P - \xi P, \end{cases} \tag{3}$$

where $\kappa = \frac{b_2}{b_1}$, $\theta_1 = \frac{s}{C_1}$, $\theta_2 = \frac{s}{C_2}$, $\gamma = \frac{\beta}{b_1 r_{A_1}}$, $\eta = \frac{s}{b_1}$, $\zeta = \frac{\alpha_1+\delta}{r_{A_1}}$, $\xi = \frac{\alpha_2}{r_{A_1}}$, and

$$S(0) = S_0 > 0, I(0) = I_0 \geq 0, P(0) = P_0 > 0. \tag{4}$$

3 Mathematical Model Analysis

The analysis of mathematical models in eco-epidemiology provides valuable insights into disease transmission dynamics, host–pathogen interactions, and the ecological feedback mechanisms within the system. Such analysis helps to explore system behavior, identify critical parameters, and examine aspects like stability, bifurcation, and possible outcomes, including disease outbreaks. Furthermore, properties such as the existence and uniqueness of solutions, positivity, boundedness, as well as permanence, persistence, and numerical simulations of the model system 3, will be studied.

3.1 Positivity of the solution

Let us denote $\mathbb{R}^3_+ = \{(S,I,P) \in \mathbb{R}^3 : S > 0, I \geq 0, P > 0\}$, the positive octants of the solution of our model system (3).

Theorem 1. *The non-negative octant in $\mathbb{R}^3$ is remain positive under the dynamics for the model (3).*

Proof. We want to verify

$$S(T) > 0, \qquad I(T) > 0, \qquad P(T) > 0, \qquad \text{for all }, T \geq 0,$$

Rewrite the system (3) in the form

$$\begin{aligned} \frac{dS}{dT} &= S\Big(1-S-\kappa I - \frac{\gamma I}{1+\eta I} - \frac{\theta_1\psi_S(S)P}{S}\Big) = SQ_1(S,I,P), \\ \frac{dI}{dT} &= I\left(\frac{\gamma S}{1+\eta I} - \zeta - \frac{\theta_2\psi_I(I)P}{I}\right) = IQ_2(S,I,P), \\ \frac{dP}{dT} &= P\left(\psi_S(S) + \psi_I(I) - \xi\right) = PQ_3(S,I,P). \end{aligned}$$

From the above expression and the initial conditions (4), we have:

$$\begin{aligned} S(T) &= S_0 \exp\left(\int_0^T Q_1(S,I,P)du\right), \\ I(T) &= I_0 \exp\left(\int_0^T Q_2(S,I,P)du\right), \\ P(T) &= P_0 \exp\left(\int_0^T Q_3(S,I,P)du\right). \end{aligned}$$

As, the initial conditions (4) and the exponential form are positive, thus, all the state variables $S(T)$, $I(T)$ and $P(T)$ are positive $\forall T \geq 0$. Therefore, every solutions of the mathematical model 3 are positive. □

3.2 Bounded behavior of trajectories

Theorem 2. *All possible solution of the dynamical system (3) are consistently bounded in $\mathbb{R}^3_+$ and enter in the invariant zone*

$$\Sigma = \left\{\Big(S(T),I(T),P(T)\Big) \in \mathbb{R}^3_+ : 0 < S \leq \max\{S_0,1\}, \right. \\ \left. 0 < \nu \leq \max\left\{\frac{(1+\xi-m)^2}{4(\xi-m)}, \nu_0\right\}\right\} \tag{5}$$

where $\nu(T) = S(T) + I(T) + \theta_1 P(T)$, $0 < \psi_I(I) \leq m$.

Proof. As established in Proposition (1), the solutions $S(T)$, $I(T)$, and $P(T)$ of system (3) remain positive for all $T \geq 0$. Considering the first equation of the model (3), it follows that

$$\frac{dS}{dT} = S\Big(1-S-\kappa I\Big) - \frac{\gamma SI}{1+\eta I} - \theta_1\psi_S(S)P \leq S(1-S)$$

This directly leads to

$$S(T) \leq \left[1 + \Big(\frac{1}{S_0} - 1\Big)e^{-T}\right]^{-1} = \frac{S_0}{S_0 + (1-S_0)e^{-T}}.$$

Therefore,

$$\lim_{T\to\infty} \sup S(T) \leq \max\{S_0, 1\}.$$

Table 1: The state variables and parameters description

Variables/Parameters	Ecological Meaning	Dimension
A_1	Susceptible prey density	Per Area
A_2	Infected prey density	Per Area
B	Predator density	Per Area
Φ_{A_1} (resp.Φ_{A_2})	Response functions	Per time
r_{A_1}	Natural propagation rate of susceptible prey	Per time
b_1	Intra-specific competition coefficient among susceptible prey	Area
b_2	Inter-specific competition coefficient between susceptible and infected prey	Area
β	Transmission rate	Per time
s	Inhibition rate	Area coverage
C_1	Proportion of susceptible prey into predator	No unit
C_2	Proportion of infected prey into predator	No unit
α_1/α_2	Natural death rates of infected prey/predator	Per time
δ	Disease induced mortality rate	Per time

Thus, $S(t)$ is bounded. To show other state variables $I(T)$ and $P(T)$ are bounded we consider

$$v = S + I + \theta_1 P$$

By differentiating v with respect to time T, we obtain

$$\begin{aligned}
\frac{dv}{dT} &= \frac{dS}{dT} + \frac{dI}{dT} + \theta_1 \frac{dP}{dT} \\
&= S\Big(1 - S - \kappa I\Big) - \frac{\gamma SI}{1+\eta I} - \theta_1 \psi_S(S)P \\
&\quad + \left(\frac{\gamma_2 SI}{1+\eta I} - \zeta I - \theta_2 \psi_I(I)P\right) \\
&\quad + \theta_1 \left(\psi_S(S)P + \psi_I(I)P - \xi P\right) \\
&= S\Big(1 - S\Big) - \kappa SI - \zeta I - \theta_2 \psi_I(I)P + \theta_1 \psi_I(I)P - \theta_1 \xi P \\
&\leq S\Big(1 - S\Big) - \kappa SI - \zeta I + \theta_1 \psi_I(I)P - \theta_1 \xi P \\
&= (1+\xi)S - S^2 - \kappa SI - (\zeta - \xi)I + \theta_1 \psi_I(I)P - \xi(S + I + \theta_1 P) \\
&\leq (1+\xi)S - S^2 + \theta_1 \psi_I(I)P - \xi v
\end{aligned}$$

The general Holling Type response function $\psi_I(I)$ is bounded, say, $\psi_I(I) \leq m$, $0 < m < \xi \leq \zeta$. Then after simplification we arrive

$$\frac{dv}{dT} \leq (1 + \xi - m)S - S^2 - (\xi - m)v \leq \frac{(1+\xi-m)^2}{4} - (\xi - m)v.$$

We can thus conclude that

$$v(T) \leq \frac{(1+\xi-m)^2}{4(\xi-m)} - \left(\frac{(1+\xi-m)^2}{4(\xi-m)} - v_0\right) e^{-(\xi-m)T}.$$

As a result, we find that

$$\lim_{T\to\infty} \sup v(T) \leq \max\left\{\frac{(1+\xi-m)^2}{4(\xi-m)}, v_0\right\}.$$

Hence, $v(T)$ remains bounded for all $T \geq 0$, which implies that the other state variables are also bounded. Consequently, all solutions of system (3) are uniformly bounded on $[0, \infty)$. □

3.3 Existence & Uniqueness

Theorem 3. *Let $F = (f_1, f_2, f_3)$. If F satisfies the Lipschitz condition and has continuous first partial derivatives with respect to x in a domain D, then $F(T, x)$ is locally Lipschitz in x. Consequently, for any initial point $(T_0, x_0) \in D$, there exists a unique solution $x(T, T_0, x_0)$ of the system*

$$\frac{dx}{dT} = F(T, x), \quad x(T_0) = x_0,$$

which passes through (T_0, x_0).

Proof. Let the right parts of the dynamical system (3) be denoted by $F = (f_1, f_2, f_3)$. Since f_1, f_2 and f_3 are continuous function, $F = (f_1, f_2, f_3)$ is continuous function in several variables, that is, $F \in C^1(\mathbb{R}^3_+)$. Thus, F satisfy the Lipschitz condition with respect to x in D. Hence, the solution of system (3) exists. The locally Lipschitz condition of F is verified using $\frac{\partial f_i}{\partial x_j}$, $i, j = 1, 2, 3$ to be continuously bounded within the domain D (Bezabih et al., 2021). We note that $F \in C^1(\mathbb{R}^3_+, Lip)$ in D and $f_1 = \frac{dS}{dT}$, $f_2 = \frac{dI}{dT}$ and $f_3 = \frac{dP}{dT}$. To show $\frac{\partial f_i}{\partial x_j}$, $i, j = 1, 2, 3$ to be continuously bounded. Now we get

$$\begin{aligned}
&\frac{\partial f_1}{\partial S} = (1 - 2S - \kappa I) - \frac{\gamma I}{1+\eta I} - \theta_1 \psi_S'(S)P \leq 1, \\
&\frac{\partial f_1}{\partial I} = -\kappa S - \frac{\gamma S}{(1+\eta I)^2} = -S\left(\kappa + \frac{\gamma S}{(1+\eta I)^2}\right), \\
&\text{This implies } \left|\frac{df_1}{dI}\right| = S\left(\kappa + \frac{\gamma S}{(1+\eta I)^2}\right) < \infty, \text{ as } S \text{ and } I \text{ are bounded,} \\
&\frac{df_1}{dP} = -\theta_1 \psi_S(S) \text{ implies } \left|\frac{df_1}{dP}\right| = \left|-\theta_1 \psi_S(S)\right| = \theta_1 \psi_S(S) < \theta_1 N_1, \\
&\qquad \text{as } \psi_S(S) \leq N_1 \in \mathbb{R}, \\
&\frac{\partial f_2}{\partial S} = \frac{\gamma I}{1+\eta I} \leq \frac{\gamma}{\eta}, \\
&\frac{\partial f_2}{\partial I} = \frac{\gamma S}{(1+\eta I)^2} - \zeta - \theta_2 \psi_I'(I)P \leq \frac{\gamma S}{(1+\eta I)^2} < \infty, \\
&\qquad \text{as } S \text{ and } I \text{ are bounded,} \\
&\frac{df_2}{dP} = -\theta_2 \psi_I(I) \implies \left|\frac{df_2}{dP}\right| = \left|-\theta_2 \psi_I(I)\right| = \theta_2 \psi_I(I) < \theta_2 N_2, \\
&\qquad \text{as } \psi_I(I) \leq N_2 \in \mathbb{R}, \\
&\frac{\partial f_3}{\partial S} = \psi_S'(S)P < \infty, \\
&\frac{\partial f_3}{\partial I} = \psi_I'(I)P < \infty, \\
&\frac{\partial f_3}{\partial P} = \psi_S(S) + \psi_I(I) - \xi < \psi_S(S) + \psi_I(I) \leq N_1 + N_2 < \infty.
\end{aligned}$$

As these all are continuous and bounded, F satisfy the locally Lipschitz condition. Therefore, the unique solution of the system (3) is verified as it is explained in Allen et al. (2007) and Hale (2009). □

3.4 Equilibrium points

The fixed points of the dynamical system (3) are the roots of a nonlinear system of equations.

$$S\Big(1 - S - \kappa I\Big) - \frac{\gamma SI}{1+\eta I} - \theta_1 \psi_S(S)P = 0, \tag{6}$$

$$\frac{\gamma SI}{1+\eta I} - \zeta I - \theta_2 \psi_I(I)P = 0, \tag{7}$$

$$\psi_S(S)P + \psi_I(I)P - \xi P = 0. \tag{8}$$

Hence, the extinction fixed point is $E^0(0,0,0)$, the axial fixed point is $E^1(1,0,0)$.
The predator free equilibrium point E^2 is obtained by the intersection point of the zero growth isocline of susceptible $\left(\frac{dS}{dT}=0\right)$ and the zero growth isocline of infected species $\left(\frac{dI}{dT}=0\right)$ where $P=0$. That is,

$$S^*\left(1 - S^* - \kappa I^*\right) - \frac{\gamma S^* I^*}{1+\eta I^*} = 0, \tag{9}$$

$$\frac{\gamma S^* I^*}{1+\eta I^*} - \zeta I^* = 0, \tag{10}$$

From equation (10), we get

$$S^* = \frac{\zeta}{\gamma} + \frac{\zeta\eta}{\gamma} I^*$$

Substitute this equation in (9), after simplification we arrived

$$\Delta_1 I^{*2} + \Delta_2 I^* + \Delta_3 = 0, \tag{11}$$

where $\Delta_1 = \eta\left(\kappa + \frac{\zeta\eta}{\gamma}\right) > 0$, $\Delta_2 = \frac{2\eta\zeta}{\gamma} + \gamma + \kappa - \eta$ and $\Delta_3 = \frac{\zeta}{\gamma} - 1$.
The positive roots I^* in the quadratic equation above is possible provided that the discriminant of an equation is positive, that is, $\Delta_2^2 - 4\Delta_1\Delta_2 > 0$ and follow from Descartes' rule of sign. We have the following results:

- If $\zeta > \gamma$ (i.e., $\Delta_3 > 0$) and $\frac{2\eta\zeta}{\gamma} + \gamma + \kappa > \eta$ (i.e $\Delta_2 > 0$), then (11) has no positive root meaning that there is no feasible equilibrium point E^2.

- If $\zeta < \gamma$ (i.e., $\Delta_3 < 0$), then there exists a unique equilibrium point E^2.

- If $\zeta > \gamma$ (i.e., $\Delta_3 > 0$) and $\frac{2\eta\zeta}{\gamma} + \gamma + \kappa < \eta$ (i.e., $\Delta_2 < 0$), then equation (11) has two positive roots, consequently two equilibrium points E_1^2, and E_2^2.

Disease free equilibrium point

The infection free fixed point of the form $E^3(S^*, 0, P^*)$ is solution of non-linear system

$$S^*\left(1 - S^*\right) - \theta_1 \psi_S(S^*)P^* = 0 \text{ and } \psi_S(S^*)P^* - \xi P^* = 0.$$

This gives $\psi_S(S^*) = \xi$ and $P^* = \dfrac{S^*\left(1-S^*\right)}{\xi\theta_1}$.

Table 2 provides an explanation of the illness free equilibrium point's existence criteria. where h is half saturation constant and w denote predator attack rate.

Table 2: Existence conditions of the disease free fixed point.

HT	HT-I	HT-II	HT-III	HT-IV
S^*	$\frac{\xi}{\omega}$	$\frac{h\xi}{\omega-\xi}$	$\sqrt{\frac{h^2\xi}{\omega-\xi}}$	$\frac{e(\omega-\xi)+\sqrt{e^2(\xi-\omega)^2-4\xi he}}{2\xi}$
Conditions	$\xi < \omega$	$h\xi < \omega - \xi$ and $\omega > \xi$	$h^2\xi < \omega - \xi$ and $\omega > \xi$	$(\xi-\omega)e > 2\sqrt{\xi h}$

The basic reproduction number, R_0

According to Layek (2015), the basic reproduction number is the average number of new infections from a single sick individual in a community that is completely susceptible over the course of the infectious period. It is used to predict whether the epidemic will spread or die out (Omar et al., 2024). To compute the basic reproduction number, we consider only the infected compartment of system (3)

$$\frac{dI}{dT} = \frac{\gamma SI}{1+\eta I} - \zeta I - \theta_2 \psi_I(I)P. \tag{12}$$

Following the next-generation matrix approach, we write

$$\frac{dI}{dT} = \mathcal{F}(I) - \mathcal{V}(I),$$

where the new infection and the transition (removal) terms represent

$$\mathcal{F}(I) = \frac{\gamma SI}{1+\eta I}, \text{ and } \mathcal{V}(I) = \zeta I + \theta_2 \psi_I(I)P.$$

Since R_0 measures the invasion of infection when I is small, we linearize the system around $I=0$. Using Taylor expansion,

$$\frac{\gamma SI}{1+\eta I} = \gamma SI(1 - \eta I + O(I^2)).$$

keeping only first-order terms gives $\mathcal{F}(I) \approx \gamma SI$. Similarly, expanding $\psi_I(I)$ near $I=0$, $\psi_I(I) \approx \psi_I'(0)I$.

Thus,

$$\mathcal{V}(I) \approx \zeta I + \theta_2 \psi_I'(0)P^* I.$$

The linearized equation becomes

$$\frac{dI}{dT} = \left[\gamma S^* - \left(\zeta + \theta_2 \psi_I'(0)P^*\right)\right] I.$$

Hence, the new infection rate is

$$F = \gamma S^*,$$

and the total removal rate is

$$V = \zeta + \theta_2 \psi_I'(0)P^*.$$

By the next-generation method,

$$R_0 = FV^{-1}.$$

Therefore,

$$R_0 = \frac{\gamma S^*}{\zeta + \theta_2 \psi_I'(0)P^*}. \tag{13}$$

Coexistence Equilibrium Point

Theorem 4. *The system admits a coexistence equilibrium $E^*(S^*, I^*, P^*)$ if the following conditions hold:*

$$S^* + \kappa I^* < 1, \quad \frac{\gamma S^*}{1+\eta I^*} > \zeta, \quad \psi_S(S^*) + \psi_I(I^*) = \xi, \quad R_0 > 1$$

.

Proof. To determine the coexistence equilibrium point $E^*(S^*, I^*, P^*)$, we set

$$\frac{dS}{dT} = 0, \qquad \frac{dI}{dT} = 0, \qquad \frac{dP}{dT} = 0.$$

Thus the equilibrium point satisfies the algebraic equations

$$S^*(1 - S^* - \kappa I^*) - \frac{\gamma S^* I^*}{1+\eta I^*} - \theta_1 \psi_S(S^*) P^* = 0, \tag{3.9}$$

$$\frac{\gamma S^* I^*}{1+\eta I^*} - \zeta I^* - \theta_2 \psi_I(I^*) P^* = 0, \tag{3.10}$$

$$\psi_S(S^*) P^* + \psi_I(I^*) P^* - \xi P^* = 0. \tag{3.11}$$

From the first, second and third equations we have $S^* + \kappa I^* < 1$, $\frac{\gamma S^*}{1+\eta I^*} > \zeta$, and $\psi_S(S^*) + \psi_I(I^*) = \xi$, respectively.
Note that

$$R_0 = \frac{\xi \theta_1 \gamma \psi_S^{-1}(\xi)}{\zeta \xi \theta_1 + \theta_2 \psi_I'(0) \psi_S^{-1}(\xi)\left(1 - \psi_S^{-1}(\xi)\right)}.$$

$$\frac{\gamma S^*}{1+\eta I^*} > \zeta \iff \frac{\gamma S^*}{\zeta(1+\eta I^*)} > 1.$$

At equilibrium (using $S^* = \psi_S^{-1}(\xi)$ we obtain

$$\frac{\gamma S^*}{\zeta(1+\eta I^*)} = R_0.$$

$$\frac{\gamma S^*}{1+\eta I^*} > \zeta \iff R_0 > 1.$$

□

4 Stability and Bifurcation Analysis

By examining sign of the derivative matrix's eigenvalues, we can determine the stability of a fixed points as in Dawed et al. (2020). The system (3) has a stable fixed point $E^*(S^*, I^*, P^*)$ if all characteristic roots of the Jacobian matrix, $J(E^*)$,

$$J(E^*) = \begin{pmatrix} J_{11} & J_{12} & J_{13} \\ J_{21} & J_{22} & J_{23} \\ J_{31} & J_{32} & J_{33} \end{pmatrix} \tag{14}$$

have negative real part where
$J_{11} = 1 - 2S^* - \kappa I^* - \frac{\gamma I^*}{1+\eta I^*} - \theta_1 \psi_S'(S^*) P^*$, $J_{12} = -\kappa S^* - \frac{\gamma S^*}{(1+\eta I^*)^2}$,
$J_{13} = -\theta_1 \psi_S(S^*)$, $J_{21} = \frac{\gamma I^*}{1+\eta I^*}$, $J_{22} = \frac{\gamma S^*}{(1+\eta I^*)^2} - \zeta - \theta_2 \psi_I'(I^*) P^*$,
$J_{23} = -\theta_2 \psi_I(I^*)$, $J_{31} = \psi_S'(S^*) P^*$, $J_{32} = \psi_I'(I^*) P^*$, and $J_{33} = \psi_S(S^*) + \psi_I(I^*) - \xi$.

The corresponding characteristic equation is $\det(J(E^*) - \lambda I_3) = 0$, that is

$$\begin{vmatrix} J_{11} - \lambda & J_{12} & J_{13} \\ J_{21} & J_{22} - \lambda & J_{23} \\ J_{31} & J_{32} & J_{33} - \lambda \end{vmatrix} = 0 \tag{15}$$

4.1 Local stability analysis

4.1.1 Stability nature near $E^0(0,0,0)$

$$J(E^0) = \begin{pmatrix} 1 & 0 & 0 \\ 0 & -\zeta & 0 \\ 0 & 0 & -\xi \end{pmatrix}$$

Thus, $\lambda_1 = 1 > 0$, $\lambda_2 = -\zeta < 0$, and $\lambda_3 = -\xi < 0$. Hence, the trivial fixed point E^0 is unstable. Biologically, this indicates that total extinction of the populations is impossible.

4.1.2 System behavior near $E^1(1,0,0)$

$$J(E^1) = \begin{pmatrix} -1 & -\kappa - \gamma & -\theta_1 \psi_S(1) \\ 0 & \gamma - \zeta & 0 \\ 0 & 0 & \psi_S(1) - \xi \end{pmatrix}$$

The eigenvalues are $\lambda_1 = -1$, $\lambda_2 = \gamma - \zeta$, and $\lambda_3 = \psi_S(1) - \xi$. Thus, the axial fixed point is locally asymptotically stable whenever $\gamma < \zeta$ and $\psi_S(1) < \xi$. This has a biological implication that susceptible prey population survive alone whenever no disease in the environment and without predator whenever the conditions holds.

4.1.3 System behavior near consumer free fixed point $E^2(S^*, I^*, 0)$

Theorem 5. *The consumer-free fixed point $E^2(S^*, I^*, 0)$ is locally asymptotically stable if the following conditions hold*

$$\begin{aligned} &(i) \quad \psi_S(S^*) + \psi_I(I^*) < \xi, \\ &(ii) \quad \zeta + 2S^* + \kappa I^* + \frac{\gamma I^*}{1+\eta I^*} < 1 + \frac{\gamma S^*}{(1+\eta I^*)^2}, \\ &(iii) \quad \left(1 - 2S^* - \kappa I^* - \frac{\gamma I^*}{1+\eta I^*}\right) \\ &\qquad \times \left(\frac{\gamma S^*}{(1+\eta I^*)^2} - \zeta\right) \\ &\qquad + \left(\kappa S^* + \frac{\gamma S^*}{(1+\eta I^*)^2}\right) \frac{\gamma I^*}{1+\eta I^*} > 0. \end{aligned}$$

Proof. The community matrix of the model (3) at E^2 is given by

$$J(E^2) = \begin{pmatrix} 1 - 2S^* - \kappa I^* - \frac{\gamma I^*}{1+\eta I^*} & -\kappa S^* - \frac{\gamma S^*}{(1+\eta I^*)^2} & -\theta_1 \psi_S(S^*) \\ \frac{\gamma I^*}{1+\eta I^*} & \frac{\gamma S^*}{(1+\eta I^*)^2} - \zeta & -\theta_2 \psi_I(I^*) \\ 0 & 0 & \psi_S(S^*) + \psi_I(I^*) - \xi \end{pmatrix}$$

The associated auxiliary equation is $det(J(E^2) - \lambda I_3) = 0$, that is

$$\begin{vmatrix} \sigma_1 - \lambda & \pi_1 & -\theta_1 \psi_S(S^*) \\ \pi_2 & \sigma_2 - \lambda & -\theta_2 \psi_I(I^*) \\ 0 & 0 & \sigma_3 - \lambda \end{vmatrix} = 0,$$

where, $\sigma_1 = 1 - 2S^* - \kappa I^* - \frac{\gamma I^*}{1+\eta I^*}$, $\sigma_2 = \frac{\gamma S^*}{(1+\eta I^*)^2} - \zeta$, $\sigma_3 = \psi_S(S^*) + \psi_I(I^*) - \xi$, $\pi_1 = -\kappa S^* - \frac{\gamma S^*}{(1+\eta I^*)^2} < 0$ and $\pi_2 = \frac{\gamma I^*}{1+\eta I^*} > 0$. Thus, one eigenvalue at $E^2(S^*, I^*, 0)$ is $\lambda_1 = \sigma_3 = \psi_S(S^*) + \psi_I(I^*) - \xi$. Now, λ_1 is negative if $\psi_S(S^*) + \psi_I(I^*) < \xi$. The rest two eigenvalues are found from the matrix

$$\bar{J}(E^2) = \begin{pmatrix} 1 - 2S^* - \kappa I^* - \frac{\gamma I^*}{1+\eta I^*} & -\kappa S^* - \frac{\gamma S^*}{(1+\eta I^*)^2} \\ \frac{\gamma I^*}{1+\eta I^*} & \frac{\gamma S^*}{(1+\eta I^*)^2} - \zeta \end{pmatrix}.$$

Using the Routh–Hurwitz criterion, the two eigenvalues of $\bar{J}$ are negative in their real parts provided that

$$\zeta + 2S^* + \kappa I^* + \frac{\gamma I^*}{1+\eta I^*} < 1 + \frac{\gamma S^*}{(1+\eta I^*)^2} \text{ and}$$
$$\left(1 - 2S^* - \kappa I^* - \frac{\gamma I^*}{1+\eta I^*}\right)\left(\frac{\gamma S^*}{(1+\eta I^*)^2} - \zeta\right) +$$
$$\left(\kappa S^* + \frac{\gamma S^*}{(1+\eta I^*)^2}\right)\frac{\gamma I^*}{1+\eta I^*} > 0.$$

Therefore, we infer that the model system (3) is locally asymptotically stable at the predator free equilibrium point E^2 as long as the conditions (i), (ii), and (iii) hold. □

4.1.4 Local Stability Near the Disease-Free Equilibrium Point

Theorem 6. *Local asymptotic stability of the infection-free fixed point $E^3(S^*, 0, P^*)$ of system (3) is ensured if the following criteria are satisfied:*

1. $R_0 < 1$,
2. $\psi_S'(S^*) > 0$,
3. $\psi_S'(S^*)(S^*)^2 - \left(2\xi + \psi_S'(S^*)\right)S^* + \xi < 0$.

Proof.

$$J(E^3) = \begin{pmatrix} \nabla_1 & -\kappa S^* - \gamma S^* & -\theta_1 \psi_S(S^*) \\ 0 & \nabla_2 & 0 \\ \psi_S'(S^*)P^* & \psi_I'(0)P^* & \nabla_3 \end{pmatrix} \quad (16)$$

where, $\nabla_1 = 1 - 2S^* - \theta_1 \psi_S'(S^*)P^*$, $\nabla_2 = \gamma S^* - \zeta - \theta_2 \psi_I'(0)P^*$ and $\nabla_3 = \psi_S(S^*) - \xi = 0$.

The associated auxiliary equation of $J(E^3)$ is

$$\begin{vmatrix} \nabla_1 - \lambda & -\kappa S^* - \gamma S^* & -\theta_1 \psi_S(S^*) \\ 0 & \nabla_2 - \lambda & 0 \\ \psi_S'(S^*)P^* & \psi_I'(0)P^* & \nabla_3 - \lambda \end{vmatrix} = 0$$

Since the matrix is block triangular with respect to the infected variable, one eigenvalue is

$$\lambda_1 = \nabla_2 = \gamma S^* - \zeta - \theta_2 \psi_I'(0)P^*.$$

Using the basic reproduction number

$$R_0 = \frac{\gamma S^*}{\zeta + \theta_2 \psi_I'(0)P^*},$$

we write

$$\lambda_1 = (\zeta + \theta_2 \psi_I'(0)P^*)(R_0 - 1).$$

Thus, if $R_0 < 1$, then $\lambda_1 < 0$ and the infection cannot invade. The others two eigenvalues are computed from the matrix

$$J = \begin{pmatrix} 1 - 2S^* - \theta_1 \psi_S'(S^*)P^* & -\theta_1 \psi_S(S^*) \\ \psi_S'(S^*)P^* & 0 \end{pmatrix}$$

By the Routh-Hurwitz stability rule, the two eigenvalues of J possess negative real parts provided that $\theta_1 \xi \psi_S'(S^*)P^* > 0$ (i.e., $\psi_S'(S^*) > 0$) and $\psi_S'(S^*)S^{*2} - (2\xi + \psi_S'(S^*))S^* + \xi < 0$. Thus, if conditions (1)–(3) are satisfied, we conclude that the model system (3) is locally asymptotically stable at the disease-free fixed point E^3. The predator eating efficiency is so high whenever conditions (1)–(3) are satisfied. The predator will only eat healthy prey because there is no infected prey present.

□

4.1.5 Global stability analysis using the Bendixson-Dulac theorem

Theorem 7. *If the Infection Free Equilibrium point $(S^*, 0, P^*)$ is locally asymptotically stable in the positive SP - plane region, then it is also globally asymptotically stable in the same region if $\frac{\psi_S(S)}{S} \geq \frac{\psi_S(S^*)}{S^*}$.*

Proof. Consequently, the system can be reduced to the following two-dimensional subsystem

$$\frac{dS}{dT} = S(1 - S) - \theta_1 \psi_S(S)P, \quad (17)$$
$$\frac{dP}{dT} = \psi_S(S)P - \xi P. \quad (18)$$

Consider $h(S, P) = \frac{1}{SP}$ as a Dulac positive function in the positive quadrant. Also, define the following functions

$$h_1(S, P) = S(1 - S) - \theta_1 \psi_S(S)P, \quad (19)$$
$$h_2(S, P) = \psi_S(S)P - \xi P. \quad (20)$$

Then,

$$\phi(S, P) = \frac{\partial}{\partial S}(h\, h_1) + \frac{\partial}{\partial P}(h\, h_2) = -\left(\frac{1}{P} + \theta_1 \frac{S\psi_S'(S) - \psi_S(S)}{S^2}\right).$$

Hence, $\phi(S, P)$ is a negative function of its arguments if $S\psi_S'(S) - \psi_S(S) \geq 0$. Note that by mean value thorem $S\psi_S'(S) - \psi_S(S) \geq 0$ and $\frac{\psi_S(S)}{S} \geq \frac{\psi_S(S^*)}{S^*}$ are equivalent. Since $\phi(S, P)$ does not change sign and is not identically zero in the positive quadrant of the SP-plane, by the Bendixson - Dulac criterion the infection free equilibrium point is globally asymptotically stable in the region

$$D = \left\{(S, P) \in R_+^2 : \frac{\psi_S(S)}{S} \geq \frac{\psi_S(S^*)}{S^*}, P > 0\right\}.$$

Moreover, the system has no limit cycle in the region. □

4.1.6 System stability conditions near endemic equilibrium point

Theorem 8. *Local asymptotic stability of the endemic equilibrium point $E^*(S^*, I^*, P^*)$ holds provided that the following conditions are met:*

(i) $D + G < 0$,
(ii) $q_1q_4 - Eq_5 + Gq_2 + Dq_3 < 0$,
(iii) $(D + G)(DG + q_2 + q_3 + Eq_4) + q_1q_4 - Eq_5 + Gq_2 + Dq_3 > 0$,

where the parameters D, E, F, and G are defined in the proof.

Proof. The positive fixed point $E^*(S^*, I^*, P^*)$ of the dynamics (3) is locally asymptotically stable if all the characteristic roots of the Jacobian matrix, J, has negative real parts, where

$$J(E^*) = \begin{pmatrix} D & -\kappa S^* - \gamma S^* F^2 & -\theta_1 \psi_S(S^*) \\ E & G & -\theta_2 \psi_I(I^*) \\ \psi_S'(S^*)P^* & \psi_I'(I^*)P^* & 0 \end{pmatrix}.$$

where, $D = 1 - 2S^* - \kappa I^* - \gamma I^* F - \theta_1 \psi_S'(S^*)P^*$, $E = \gamma I^* F$, $F = \dfrac{1}{1+\eta I^*}$ and $G = \gamma S^* F^2 - \zeta - \theta_2 \psi_I'(I^*)P^*$.

The characteristic equation is

$$\begin{vmatrix} D - \lambda & -\kappa S^* - \gamma S^* F^2 & -\theta_1 \psi_S(S^*) \\ E & G - \lambda & -\theta_2 \psi_I(I^*) \\ \psi_S'(S^*)P^* & \psi_I'(I^*)P^* & -\lambda \end{vmatrix} = 0$$

This implies

$$\lambda^3 + k_1\lambda^2 + k_2\lambda + k_3 = 0 \tag{21}$$

where, $k_1 = -(D + G)$, $k_2 = DG + q_2 + q_3 + Eq_4$, $k_3 = -(q_1q_4 - Eq_5 + Gq_2 + Dq_3)$, $q_1 = \theta_2\psi_I(I^*)\psi_S'(S^*)P^*$, $q_2 = \theta_1\psi_S(S^*)\psi_S'(S^*)P^*$, $q_3 = \theta_2\psi_I(I^*)\psi_I'(I^*)P^*$, $q_4 = \kappa S^* + \gamma S^* F^2$ and $q_5 = \theta_1\psi_S(S^*)\psi_I'(I^*)P^*$. Consequentially, if $D+G < 0$, then $k_1 > 0$. If $q_1q_4 - Eq_5 + Gq_2 + Dq_3 < 0$, then $k_3 > 0$. Moreover, $k_1k_2 - k_3 > 0$ if $(D + G)(DG + q_2 + q_3 + Eq_4) + q_1q_4 - Eq_5 + Gq_2 + Dq_3 > 0$. According to the Routh–Hurwitz criterion, the model system 3 is locally asymptotically stable at the endemic fixed point $E^* = (S^*, I^*, P^*)$ if the corresponding conditions are satisfied. □

4.2 Local bifurcation analysis

Bifurcations analysis helps to predict and understand transitions in the behavior of dynamical system as parameters value change. Local bifurcation refers, change in the qualitative behavior of dynamical system near fixed point as a system's parameters are varied.

Theorem 9. *(Transcritical Bifurcation)*

1. *The diseased model (3) demonstrate a transcritical bifurcation at parameter values $\zeta = \zeta^{[1]} = \gamma$ or $\xi = \xi^{[2]} = \psi_S(1)$ in the neighborhood of the equilibrium point $E^1(1, 0, 0)$.*

2. *When the parameter ξ attains the bifurcation threshold $\hat{\xi} = \psi_S(S^*) + \psi_I(I^*)$, the system (3) near the equilibrium $E^2(S^*, I^*, 0)$ exhibits*

   (i). No saddle-node bifurcation occurs but

   (ii). A transcritical bifurcation is observed.

Proof. (1). Consider the community matrix of model (3) evaluated at $E^1(1, 0, 0)$:

$$J(E^1) = \begin{pmatrix} -1 & -(\kappa + \gamma) & -\theta_1\psi_S(1) \\ 0 & \gamma - \zeta & 0 \\ 0 & 0 & \psi_S(1) - \xi \end{pmatrix}.$$

The eigenvalues of $J(E^1)$ are $\lambda_1 = -1 < 0$, $\lambda_2 = \gamma - \zeta$, and $\lambda_3 = \psi_S(1) - \xi$. Therefore, E^1 is locally asymptotically stable provided that $\gamma < \zeta$ and $\psi_S(1) < \xi$ hold. Substituting either $\zeta = \gamma$ or $\xi = \psi_S(1)$ into $J(E^1)$ yields a zero eigenvalue in the characteristic equation.

With $\zeta = \zeta^{[1]}$, the eigenvectors V and W, associated with the zero eigenvalue of the Jacobian $J^{[1]}(E^1, \zeta^{[1]})$ and its transpose, respectively, are

$$V = \begin{pmatrix} -(\kappa + \gamma)a \\ a \\ 0 \end{pmatrix}, \quad W = \begin{pmatrix} 0 \\ b \\ 0 \end{pmatrix},$$

where $a, b \neq 0$. The derivative of the vector field $F(S, I, P) = (F_1, F_2, F_3)^T$ with respect to ζ is

$$F_\zeta(X, \zeta) = \begin{pmatrix} 0 \\ -I \\ 0 \end{pmatrix}, \quad F_\zeta(E^1, \zeta^{[1]}) = \begin{pmatrix} 0 \\ 0 \\ 0 \end{pmatrix},$$

implying

$$W^T F_\zeta(E^1, \zeta^{[1]}) = 0.$$

Hence, the first condition of Sotomayor's theorem Pirayesh et al., 2016 for a transcritical bifurcation is met.

Next, we compute

$$DF_\zeta(E^1, \zeta^{[1]}) = \begin{pmatrix} 0 & 0 & 0 \\ 0 & -1 & 0 \\ 0 & 0 & 0 \end{pmatrix}, \quad DF_\zeta(E^1, \zeta^{[1]})V = \begin{pmatrix} 0 \\ -a \\ 0 \end{pmatrix},$$

so that

$$W^T[DF_\zeta(E^1, \zeta^{[1]})V] = -ab \neq 0.$$

Finally, the second derivative of F along V is

$$D^2F(E^1, \zeta^{[1]})(V, V) = \begin{pmatrix} -2v_1^2 + 2\gamma\eta v_2^2 + 2(-\kappa - \gamma)v_1v_2 \\ -2\gamma\eta v_2^2 + 2\gamma v_1 v_2 \\ 0 \end{pmatrix},$$

giving

$$W^T[D^2F(E^1, \zeta^{[1]})(V, V)] = -2b\zeta(\eta v_2^2 - v_1v_2) \neq 0 \quad \text{whenever } \eta v_2 \neq v_1.$$

Therefore, by Sotomayor's theorem Pirayesh et al., 2016; Yu et al., 2020, the model (3) demonstrate transcritical bifurcation at $\zeta = \zeta^{[1]}$ near the axial fixed point $E^1(1, 0, 0)$ provided that $\eta v_2 \neq v_1$.

Now, let us examine the bifurcation at $\xi = \xi^{[2]} = \psi_S(1)$. The eigenvectors V and W, associated to the zero eigenvalues of the matrices $J^{[2]}(E^1, \xi^{[2]})$ and its transpose respectively, can be written as

$$V = (v_1 \quad v_2 \quad v_3)^T = (-\theta_1\psi_S(1) \quad 0 \quad c)^T \text{ and } W = (0 \quad 0 \quad d)^T$$

where c and d are nonzero real numbers. It follows that

$$F_\xi(X, \xi) = \begin{pmatrix} 0 \\ 0 \\ -P \end{pmatrix}, \quad F_\zeta(E^1, \xi^{[2]}) = \begin{pmatrix} 0 \\ 0 \\ 0 \end{pmatrix}.$$

This implies that, $W^T F_\xi(E^1, \xi^{[2]}) = 0$. Moreover,

$$DF_\xi(E^1, \xi^{[2]}) = \begin{pmatrix} 0 & 0 & 0 \\ 0 & 0 & 0 \\ 0 & 0 & -1 \end{pmatrix},$$

$$\mathrm{DF}_\xi(E^1, \xi^{[2]})V = \begin{pmatrix} 0 & 0 & 0 \\ 0 & 0 & 0 \\ 0 & 0 & -1 \end{pmatrix}\begin{pmatrix} -\theta_1\psi_S(1)c \\ 0 \\ c \end{pmatrix} = \begin{pmatrix} 0 \\ 0 \\ -c \end{pmatrix}.$$

Hence, $W^T[DF_\xi(E^1,\xi^{[2]})V] = -cd \neq 0$. Furthermore,

$$D^2F(E^1,\xi^{[2]})(V,V) = \begin{pmatrix} -2v_1^2 - 2\theta_1\psi_S'(1)v_1v_3 \\ 0 \\ 2\psi_S'(1)v_1v_3 \end{pmatrix}$$

which implies that,

$$W^T[D^2F(E^1,\xi^{[2]})(V,V)] = 2\psi_S'(1)v_1v_3 = -2dc^2\theta_1\xi\psi_S'(1) \neq 0.$$

Hence, based on the Sotomayor's theorem as in Pirayesh et al. (2016) and Yu et al. (2020) the model exhibit transcritical bifurcation at $\xi = \xi^{[2]} = \psi_S(1)$ near to the axial equilibria $E^1(1,0,0)$.
See the proof of (2) in the appendix A. □

Theorem 10 (Hopf Bifurcation). *The system undergoes a Hopf bifurcation near to the equilibrium point $E^2(S^*,I^*,0)$ at the parameter value $\eta = \eta^*$, provided the following criteria are hold:*

1. *At $\eta = \eta^*$, we have $D_1 = 0$ and $D_2 > 0$, which guarantees the existence of a pair of purely imaginary eigenvalues, and*
2. *The transversality condition is satisfied, i.e.,*

$$\Re\left(\frac{d\lambda_j}{d\eta}\right)_{\eta=\eta^*} \neq 0, \quad j = 2,3,$$

where λ_j denote the eigenvalues of the auxiliary equation

$$\lambda^2 + D_1\lambda + D_2 = 0$$

associated with E^2. Here, $D_1 = -(\sigma_1+\sigma_2)$ and $D_2 = \sigma_1\sigma_2 - \pi_1\pi_2$, with σ_i and π_i $(i = 1,2)$ defined in the proof part.

Proof. The auxiliary equation of the model (3) at E^2 is

$$\begin{vmatrix} \sigma_1 - \lambda & \pi_1 & -\theta_1\psi_S(S^*) \\ \pi_2 & \sigma_2 - \lambda & -\theta_2\psi_I(I^*) \\ 0 & 0 & \sigma_3 - \lambda \end{vmatrix} = 0,$$

where, $\sigma_1 = 1 - 2S^* - \kappa I^* - \frac{\gamma I^*}{1+\eta I^*}$, $\sigma_2 = \frac{\gamma S^*}{(1+\eta I^*)^2} - \zeta$, $\sigma_3 = \psi_S(S^*) + \psi_I(I^*) - \xi$, $\pi_1 = -\kappa S^* - \frac{\gamma S^*}{(1+\eta I^*)^2} < 0$ and $\pi_2 = \frac{\gamma I^*}{1+\eta I^*} > 0$. After simplification

$$(\sigma_3 - \lambda)(\lambda^2 + D_1\lambda + D_2) = 0 \tag{22}$$

where

$$D_1 = -(\sigma_1+\sigma_2) = -\left(1 - 2S^* - \kappa I^* - \frac{\gamma I^*}{1+\eta I^*} + \frac{\gamma S^*}{(1+\eta I^*)^2} - \zeta\right),$$

$$D_2 = \sigma_1\sigma_2 - \pi_1\pi_2 = \left(1 - 2S^* - \kappa I^* - \frac{\gamma I^*}{1+\eta I^*}\right)\left(\frac{\gamma S^*}{(1+\eta I^*)^2} - \zeta\right) + \left(\kappa S^* + \frac{\gamma S^*}{(1+\eta I^*)^2}\right)\frac{\gamma I^*}{1+\eta I^*}.$$

Eq'n (22) has pure imaginary roots if $D_1 = 0$ and $D_2 > 0$ from which the threshold value $\eta = \eta^*$. Thus, when $\eta = \eta^*$, $\lambda_1 = \sigma_3$, $\lambda_2 = i\sqrt{D_2}$, and $\lambda_3 = -i\sqrt{D_2}$. Differentiating equation (22) with respect to η, we have

$$2\lambda\frac{d\lambda}{d\eta} + \lambda\frac{dD_1}{d\eta} + D_1\frac{d\lambda}{d\eta} + \frac{dD_2}{d\eta} = 0.$$

This implies that, $\frac{d\lambda}{d\eta} = -\frac{\dot{D}_2 + \lambda\dot{D}_1}{D_1 + 2\lambda}$. Thus, at $\eta = \eta^*$ it is reduced to

$$\left[\frac{d\lambda}{d\eta}\right]_{\eta=\eta^*} = -\left[\frac{\dot{D}_2 + \lambda\dot{D}_1}{D_1 + 2\lambda}\right]_{\lambda=i\sqrt{D_2}} = \frac{-\dot{D}_1\sqrt{D_2}}{2D_2} + i\frac{\dot{D}_2\sqrt{D_2}}{2D_2}.$$

Hence, $Re\left[\frac{d\lambda_j}{d\eta}\right]_{\eta=\eta^*} = -\frac{\dot{D}_1\sqrt{D_2}}{2D_2} \neq 0$.
Hence, the transversality condition

$$\Re\left(\frac{d\lambda_j}{d\eta}\right)_{\eta=\eta^*} \neq 0, \quad j = 2,3,$$

is satisfied, which confirms the occurrence of a Hopf bifurcation at $\eta = \eta^*$. Furthermore, it can be demonstrated that there exists a threshold value of the parameter γ at which the present model also demonstrate a stability switch via Hopf bifurcation.

□

Theorem 11. *If the bifurcation parameter is given by*

$$\zeta^{[0]} = \frac{\theta_1\xi\gamma_2 S - \theta_2\psi_I'(0)S(1-S)}{\theta_1\xi},$$

then the model system (3) at the infection-free fixed point $E^3(S^*,0,P^*)$ does not exhibit a saddle-node bifurcation. Instead, the transcritical bifurcation of the system is observed. See the proof in the appendix B.

5 Computational Analysis

In order to validate the theoretical results, the researchers numerically explore the dynamic behavior of their model using the `ode45` solver in MATLAB. Owing to the unavailability of empirical data, a biologically feasible and representative set of parameter values is adopted for the purpose of numerical simulations. $X = \{\alpha_1 = 0.001, \alpha_2 = 0.007, \gamma = 2.5, \theta_1 = 0.04, \theta_2 = 0.02, \zeta = 0.04, \kappa = 1.3, \xi = 0.01, \eta = 0.03, h = 0.064,$ and $e = 0.05\}$. Moreover, for simulation purposes, we consider four representative models selected from the sixteen possible combinations of Holling-type functional responses. Specifically:

- **Model 1:** Represents the disease model with(HT-I–HT-II).
- **Model 2:** Corresponds to the combination (HT-II–HT-III).
- **Model 3:** Defined by the combination (HT-III–HT-II).
- **Model 4:** Represents the combination (HT-IV–HT-III).

These four sample models are selected as representative cases among the sixteen Holling-type response function combinations to capture different nonlinear interaction mechanisms and to compare their qualitative impacts on the disease transmission dynamics. When the consumer species is absent in the dynamics 3, then the model is dominated by prey population. The time-series plots in Figure (1) show that both $S(t)$ and $I(t)$ converge smoothly to their fixed point values $E^2(S^*,I^*,0)$, indicating local asymptotic stability. The infected prey population increases initially due to infection transmission, then stabilizes at a moderate level, while the susceptible population decreases and reaches a steady state.

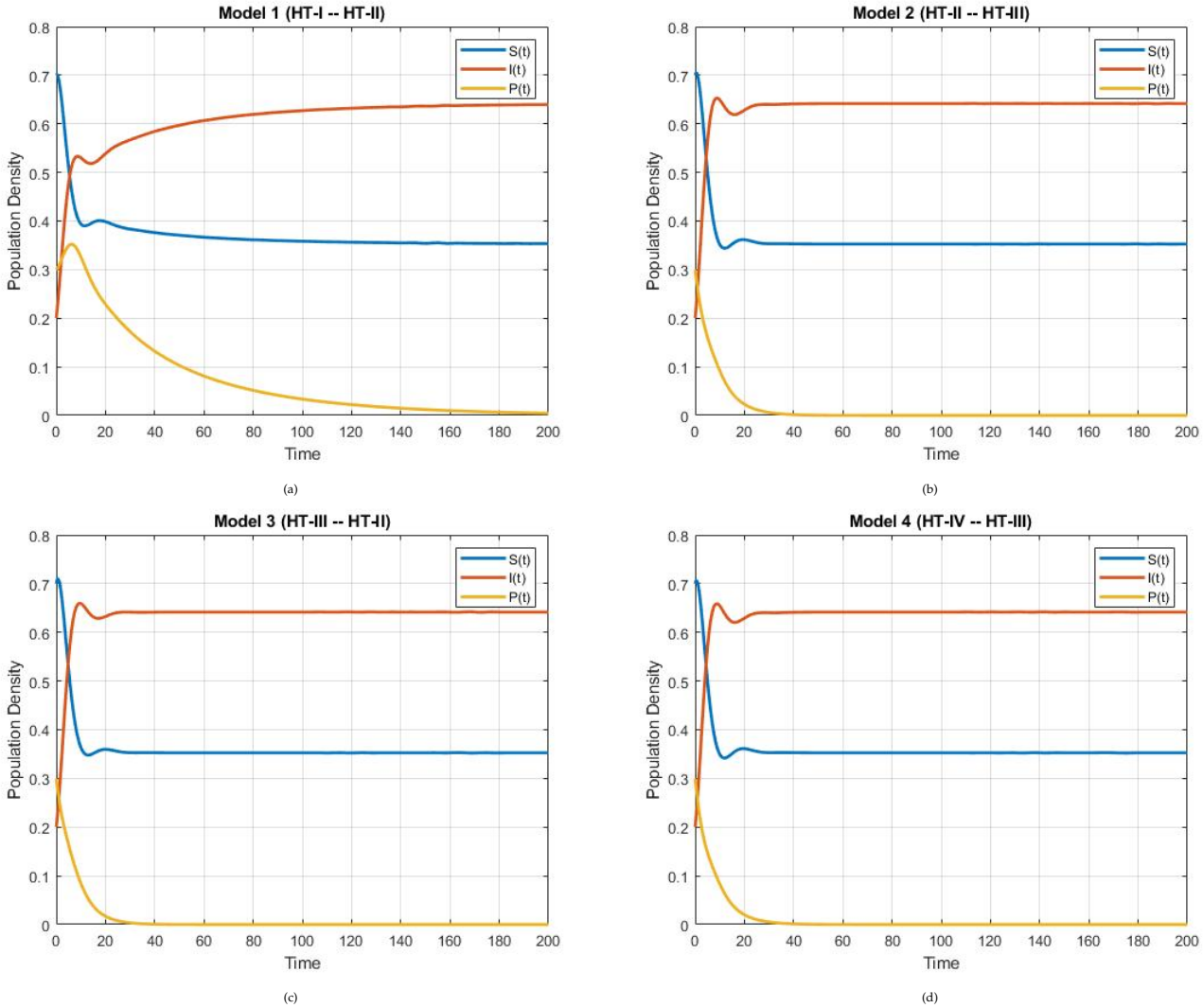

Figure 1: Time series plot of the system (3), where the parametric values $\kappa = 0.3$; $\gamma = 0.8$; $\eta = 0.2$; $\theta_1 = 0.4$; $\theta_2 = 0.3$; $\zeta = 0.25$; $xi = 0.5$; $a_1 = 0.6$; $a_2 = 0.5$; $b_1 = 0.4$; $b_2 = 0.3$; $c_1 = 0.2$; and initial condition $(0.70,\ 0.120,\ 0.3)$.

When host is absent in the model system (3), the dynamics reduce to a predator-prey subsystem involving S and P. In Figure (2) the time series plots show both populations converging to the host-free fixed point $E^3(S^*, 0, P^*)$. Consumers grow up initially fueled by prey availability, then stabilize as prey density decreases. Additionally, the phase diagrams confirm that trajectories approach the subspace $I = 0$. The infection-free fixed point is locally asymptotically stable under the parameter sets considered, consistent with Theorem 6.

Figure 3 shows the system dynamics begin with periodic oscillation and through time it goes to a locally asymptotically stable endemic fixed point, where the computational laboratory is performed for some possible Holling Type response function combinations of the mathematical Eco-Epidemiology model for the diseased-model (3).

Overall, the simulations show that both predator-free and disease-free equilibria are stable, while nonlinear functional responses mainly affect the rate and amplitude of transient dynamics rather than the final steady state. These results emphasize the regulatory roles of infection and predation in prey dynamics and the stabilizing influence of functional response saturation.

The bifurcation diagrams in Figures 4 confirm the predicted transcritical bifurcations in system (3) (Theorem 9). As the parameter ζ cross its thresholds, equilibria exchange stability, with the infected equilibrium I^* smoothly transitioning from stable to unstable.

Ecologically, small changes in disease-induced mortality ζ can shift the system between disease-free and infected states, or from predator extinction to coexistence, reflecting the influence of nonlinear functional responses ψ_S and ψ_I.

Models 1 and 2 show bifurcations at lower thresholds, indicating higher sensitivity and faster infection spread under simpler responses. In contrast, Models 3 and 4, show stronger saturation or complex predation terms, display delayed transitions, highlighting greater ecological resilience.

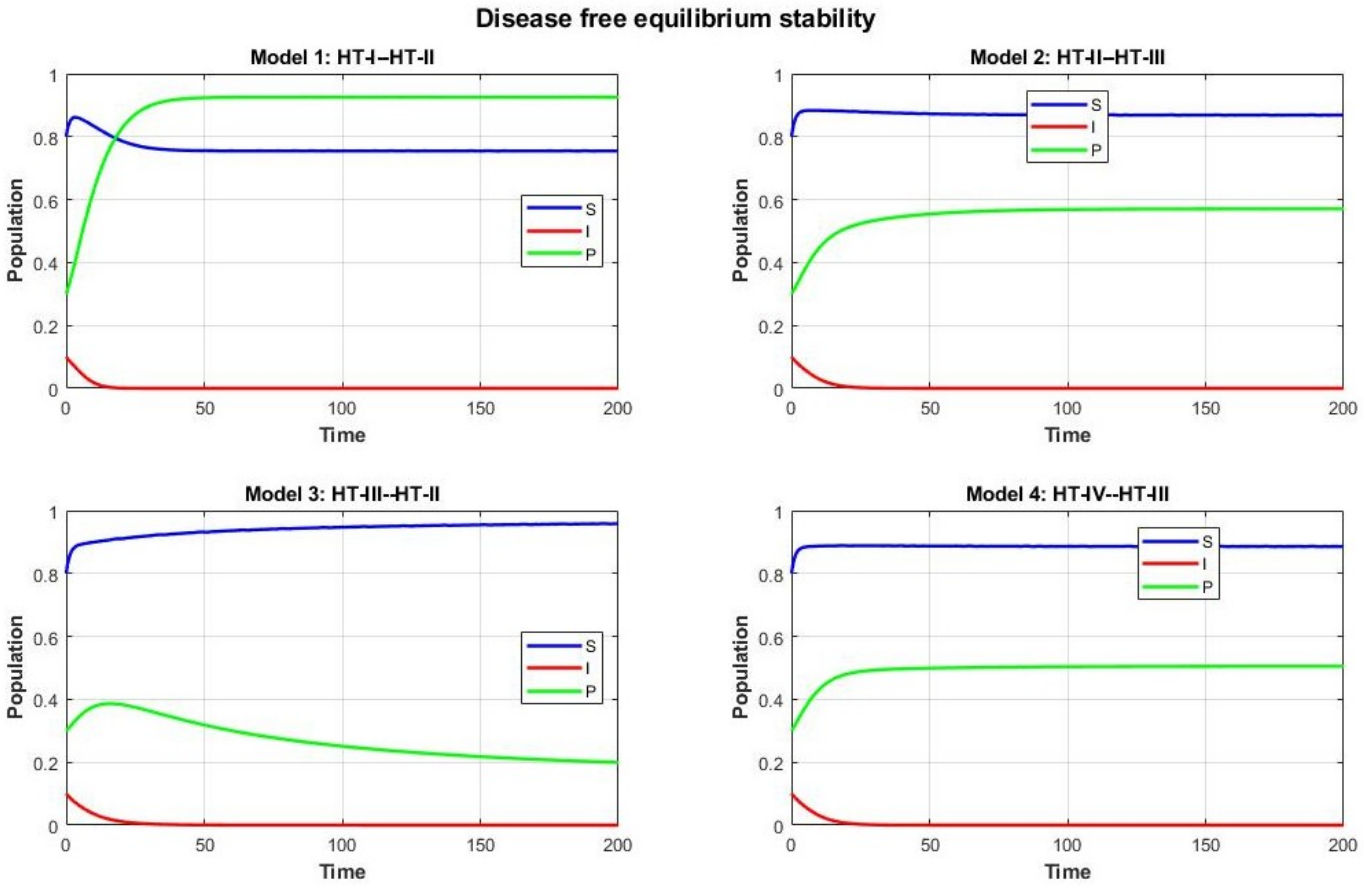

Figure 2: Time series plot of the system (3), where the parametric values $\kappa = 0.10$; $\gamma = 0.4$; $\eta = 0.10$; $\zeta = 0.30$; $\theta_1 = 0.50$; $\theta_2 = 0.70$; $\xi = 0.40$; $a = 0.65$; $b = 0.3$; $h = 0.20$; $h_1 = 0.30$; $h_2 = 0.25$; and initial condition $(0.80,\ 0.1,\ 0.3)$.

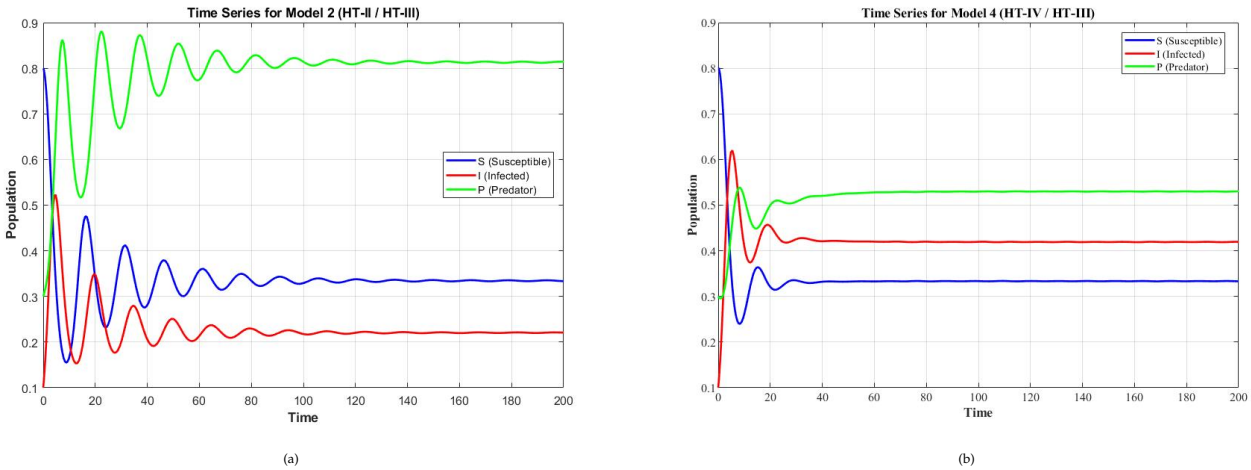

(a) (b)

Figure 3: Time seires plot of the model system 3, where the parameter values $\gamma = 1.2$, $\theta_1 = 0.5$, $\theta_2 = 0.3$, $\zeta = 0.3$, $\kappa = 0.1$, $\xi = 0.4$, $a = 0.6$, $b = 0.3$, $c = 0.2$, $\eta = 0.03$, $h_1 = 0.3$, $h_2 = 0.25$ and for the, initial condition $(0.8, 0.1, 0.3)$.

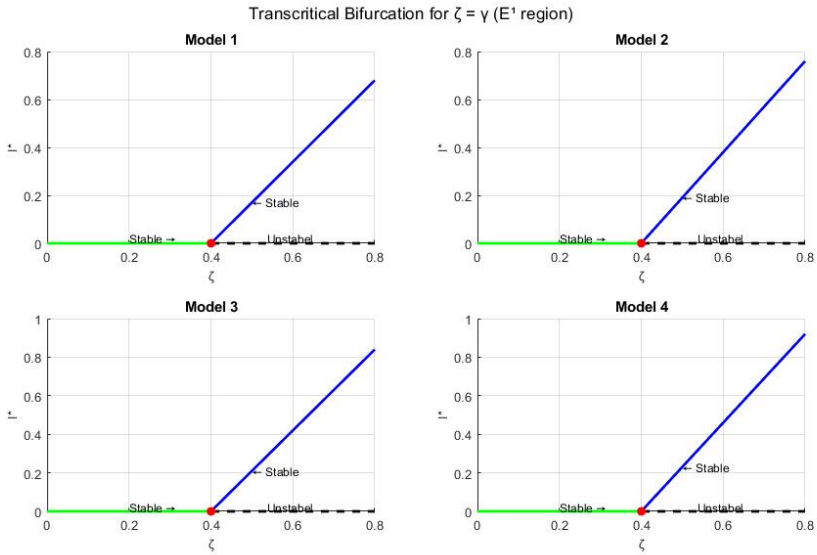

Figure 4: Bifurcation diagrams for Models 1–4 with respect to $\zeta = \gamma$ near the equilibrium $E^1(1, 0, 0)$. The horizontal axis represents the bifurcation parameter ζ, and the vertical axis represents the infected equilibrium I^*. Solid lines denote stable equilibria, while dashed lines denote unstable equilibria and the bifurication value is $\zeta = 0.4$.

5.1 Impact of the inhibition rate, η

The inhibition rate η appears in the infection term which regulates the rate at which susceptible prey become infected. From Figure(5), the parameter η controls the saturation level of the infection process for small values of η, the incidence rate is almost linear in I, leading to rapid spread of infection; for large η, the infection saturates quickly, representing inhibitory effects such as crowding, limited contact, or behavioral avoidance. Ecologically, η represents density-dependent inhibition in the infection process due to immunity, crowding, or behavioural avoidance among prey. As η increases, the effective contact rate between susceptible and infected prey decreases, reducing infection pressure. This reduction weakens the oscillatory feedback between prey and predator populations, thereby promoting stability in the coexistence equilibrium.

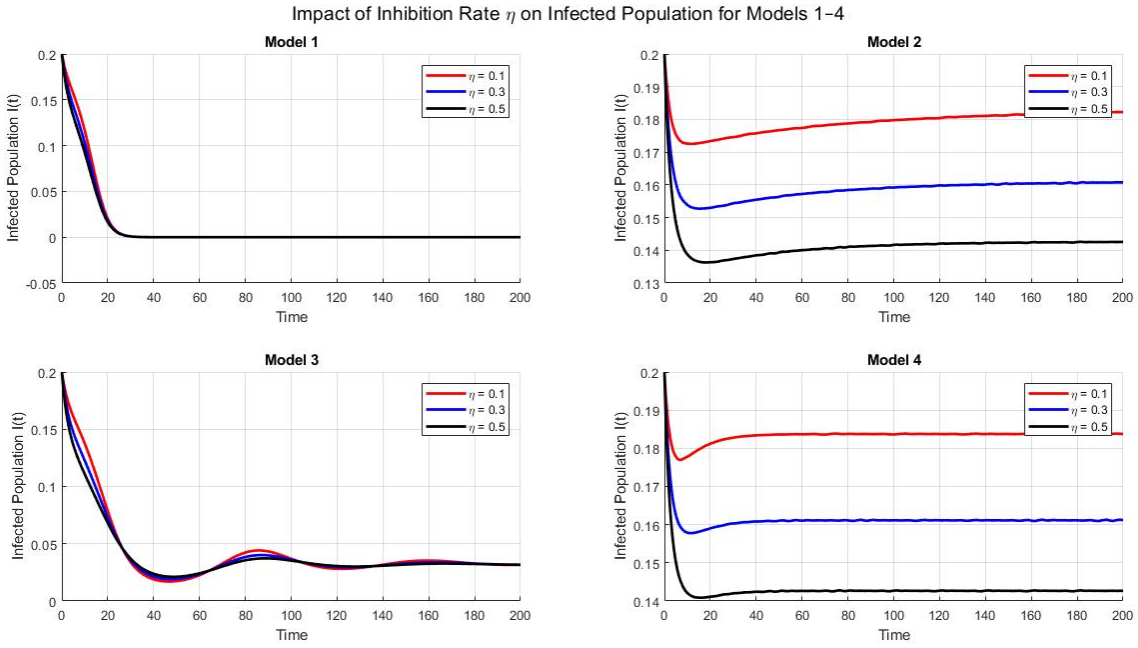

Figure 5: Time series showing the impact of the inhibition rate η on system stability for HT-II–HT-III, where parameters value $\eta = 0.1,\ 0.3,\ 0.5, \kappa = 0.5; \gamma = 0.8; \theta_1 = 0.2;$ $\theta_2 = 0.15; \zeta = 0.6; \xi = 0.5; a = 0.6; b = 0.3; c = 0.2;$ and initial condition $(0.7,\ 0.2,\ 0.1)$.

5.2 Impact of the transmission rate, γ

As illustrated in Figure 6, the transmission parameter γ has also have a signification effect on the dynamical behaviour of population I , and as transmission rates γ increasing the infected prey population rise up, and making the nature of stability of the coexistence equilibrium is becomes more periodic and take long time to stable. Moreover, for different Holling Type response functions combination, the patterns of stability of endemic equilibrium point are identical.

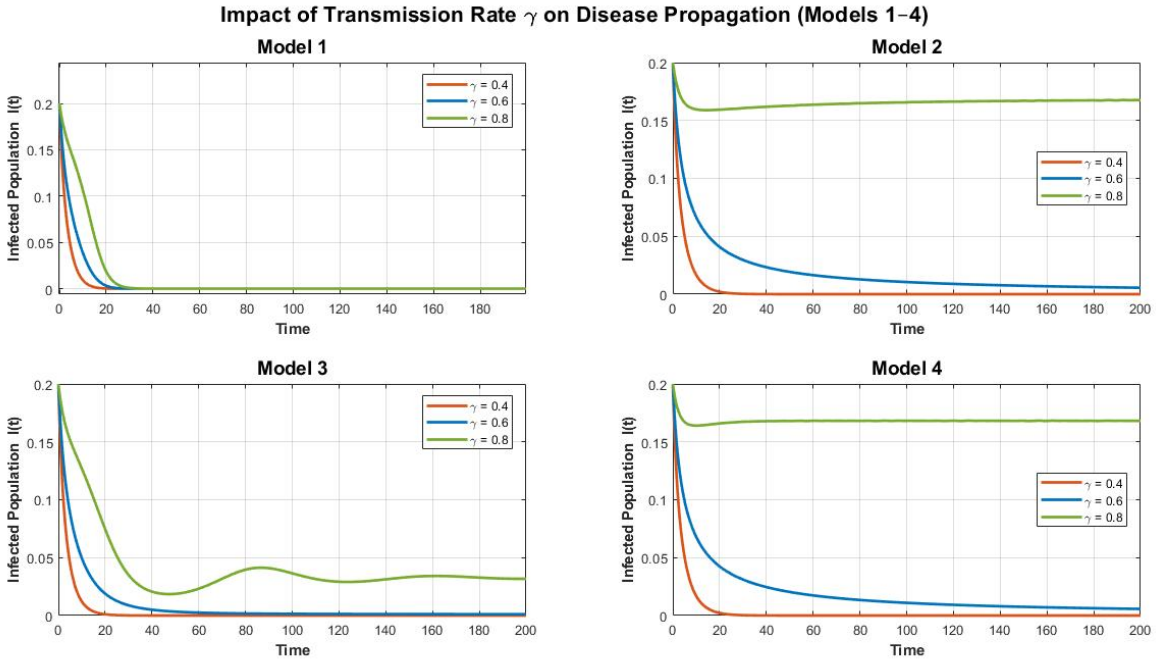

Figure 6: Time series plot of the dynamical system (3) for different values of transmission rate $\gamma = 0.4,\ 0.6,\ 0.8$ for Mode 1-4, where other parameter values $\kappa = 0.5$, $\eta = 0.3$, $\theta_1 = 0.2$, $\theta_2 = 0.15$, $\zeta = 0.6$, $\xi = 0.5$; $a = 0.6$; $b = 0.3$; $c = 0.2$ and initial condition $(0.7,\ 0.2,\ 0.1)$.

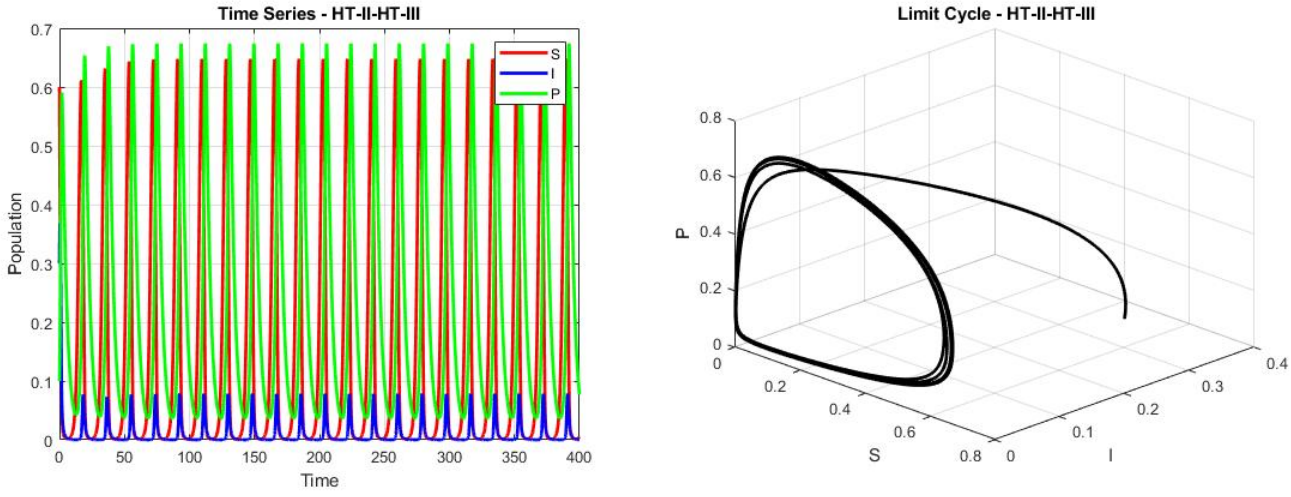

(a) (b)

Figure 7: Time series plot(periodic solution) and phase diagram (limit cycle) of the model system HT-II–HT-III, where the parameter values $\kappa = 0.4$, $\gamma = 5.0$, $\zeta = 0.6$, $\theta_1 = 1.2$, $\theta_2 = 1.0$, $a_1 = 1.5$, $a_2 = 1.3$, $b = 0.4$, $h = 0.2$, $\xi = 0.3$, $\eta = 2.0$, and initial condition (0.6, 0.3, 0.1).

Figure 7 indicates existence of Hopf bifurcation which verifies Theorem 4.6. Ecologically, η measures the strength of inhibitory (saturation) effects regulating predation or disease transmission. For $\eta < \eta^*$, the populations coexist at a stable steady state. When $\eta > \eta^*$, the equilibrium loses stability and sustained oscillations emerge due to feedback between infection spread and predation pressure. Increased infection enhances predator growth, which subsequently suppresses the host population, leading to predator decline and eventual host recovery. This recurring mechanism generates persistent population cycles, reflecting realistic eco-epidemiological fluctuations observed in natural ecosystems.

6 Result

In this section, we concisely summarize the main analytical and numerical findings obtained in Sections 4 and 5 for the eco-epidemiological model (3). The local and global stability conditions of all equilibrium points, corresponding to different combinations of Holling-Type functional responses, are presented in Table (3). These results establish the parametric regimes under which the system exhibits disease-free, endemic, predator-free, or coexistence states.

The bifurcation analysis results of the eco-epidemiological dynamics 3 near equilibrium points are summarized in table (4).

Table 3: Stability analysis result of Equilibrium points of the model system 3: Note; LAS ≡ locally asymptotically stable, GAS ≡ globally asymptotically stable

Equilibria	Stability conditions	Stability status
E^0	Always	Unstable
E^1	$\gamma < \zeta$ and $\psi_S(1) = \zeta$	LAS
E^2	Conditions stated in Theorem (5) (i)–(iii)	LAS
E^3	Conditions stated in Theorem (6) (1)–(3)	LAS
E^3	$\psi_S(S) \geq \exp \int_0^T \frac{du}{S}$	GAS
E^*	Conditions stated in Theorem (8)(i)–(iii)	LAS

The collective results depicted in Figures 4 clearly demonstrate how variations in the key bifurcation parameter ζ regulate the coexistence and persistence of prey, infected prey, and predator populations. The transcritical bifurcation marks a critical threshold where the system shifts from a disease-free to an endemic equilibrium, reflecting a change in ecological stability and disease prevalence.

From an ecological perspective, increasing the recovery rate (ξ) helps drive the system toward a disease-free state. Comparing Models 1–4, introducing nonlinear saturation in infection and predation stabilizes the system by postponing bifurcations. This highlights the importance of using realistic functional responses in eco-epidemiological models to capture key biological feedbacks and better understand ecosystem resilience under disease pressure.

Table 4: Local bifurcation analysis result of Equilibrium points of the model 3: TB ≡ Transcritical bifurcation, HB ≡ Hopf bifurcation

E.P	**Threshold value**	**Stability condition**	**Bifurcation**
E^1	$\gamma = \zeta$	$\eta v_2 \neq v_1$	TB
E^1	$\psi_S(1) = \xi$	always	TB
E^2	$\hat{\xi} = \psi_S(S^*) + \psi_I(I^*)$	$\psi_S'(S^*)V_1 + \psi_I'(I^*)V_2 \neq 0$	TB
E^2	$\eta = \eta^*$	$D_1 = 0, D_2 > 0$ and $Re\left[\frac{d\lambda_j}{d\eta}\right]_{\eta=\eta^*} \neq 0$	HB
E^3	$\zeta^{[0]} = \frac{\theta_1\xi\gamma_2 S - \theta_2\psi_I'(0)S(1-S)}{\theta_1\xi}$	$-(2\gamma\eta S^* + \theta_2\psi_I''(0)P^*)V_2^2\Upsilon + 2(\gamma V_1 V_2\Upsilon - \theta_2\psi_I'(0)V_2V_3)\Upsilon \neq 0$	TB

The inhibition (saturation) parameter η plays a critical regulatory role. When η is below the critical threshold ($\eta^* = 2$), the system settles into a stable coexistence of susceptible prey, infected prey, and predators. However, once η exceeds this value, a Hopf bifurcation occurs: the equilibrium becomes unstable and a stable limit cycle emerges. Biologically, this leads to recurring oscillations driven by feedback between disease transmission and predation. Increased susceptible prey boosts infection and predator growth; predators then reduce prey populations, which in turn lowers predator numbers, allowing prey to recover and restarting the cycle.

Overall, the Hopf bifurcation shows how changes in inhibitory effects can shift the ecosystem from stable coexistence to sustained oscillations, underscoring the delicate balance between disease dynamics and predator–prey interactions.

7 Conclusion

In this study, the researchers have investigated an eco-epidemiological mathematical model in which a prey population is infected by microparasites, while predators feed on both susceptible and infected prey following a general Holling-type functional response. The model was developed to explore how disease transmission and predation efficiency affect the overall community structure and population dynamics. An emergent carrying capacity was introduced to reflect the fact that infected prey, having reduced fitness, are more easily captured by predators. The stability and bifurcation conditions were derived for different equilibrium points, including trivial, axial, predator-free, disease-free, and endemic states. Analytical and numerical analyses showed strong agreement between theoretical predictions and simulation results.

The system exhibits oscillatory behavior for lower values of the inhibition rate (η), whereas higher inhibition rates promote stability. Hopf bifurcation analysis, taking η as the bifurcation parameter, revealed that increasing inhibition enhances system stability. Furthermore, when the predation rates (ω_1, ω_2) exceed a critical threshold, the predator-free equilibrium becomes unstable, and a stable disease-free coexistence of prey and predator emerges. The bifurcation analysis indicates that disease transmission and predator–prey interactions jointly determine ecosystem stability. Managing infection parameters such as the transmission rate can prevent oscillatory outbreaks and species extinction. Hence, controlling ecological feedbacks through parameter tuning plays a crucial role in maintaining biodiversity and long-term coexistence within predator–prey systems. Overall, the theoretical and numerical investigations are carried out under saturating incidence rates demonstrate the biological consistency of the proposed model. The results provide valuable insights into the interplay between infection, predation efficiency, and population stability in eco-epidemiological systems. The primary contribution of this work lies in providing a comprehensive bifurcation analysis under these combined nonlinear mechanisms. We rigorously establish threshold dynamics through the basic reproduction number and employ bifurcation theory to demonstrate the occurrence of transcritical and Hopf bifurcations. The results reveal how inhibition and transmission parameters govern transitions between disease-free equilibria, endemic coexistence, and sustained oscillatory outbreaks.

Future studies can extend this work by incorporating time delays representing disease incubation or predator gestation periods, which may lead to more complex dynamical behaviors such as chaos or multiple attractors. Furthermore, integrating stochastic effects, seasonal

variations, or optimal control strategies may enhance the model applicability to real-world ecological management and conservation policies.

Data Availability Statement

The data supporting the findings of this study are available from the authors upon reasonable request.

Conflicts of interest

The authors declare that they have no conflicts of interest relevant to this study.

Author Contributions

All have equal contribution.

Funding

This research received no specific grant from any funding agency.

References

Allen, L. J., Bolker, B. M., Lou, Y., & Nevai, A. L. (2007). Asymptotic profiles of the steady states for an sis epidemic patch model. *SIAM Journal on Applied Mathematics*, *67*(5), 1283–1309.

Anderson, R. M., & May, R. M. (1986). The invasion, persistence and spread of infectious diseases within animal and plant communities. *Philosophical Transactions of the Royal Society of London. B, Biological Sciences*, *314*(1167), 533–570.

Bezabih, A. F., Edessa, G. K., & Rao, K. P. (2021). Mathematical modeling the impact of infectious diseases in prey-predator interactions.

Biswas, S., Samanta, S., & Chattopadhyay, J. (2015). A model based theoretical study on cannibalistic prey–predator system with disease in both populations. *Differential Equations and Dynamical Systems*, *23*, 327–370.

Brauer, F. (2005). The kermack–mckendrick epidemic model revisited. *Mathematical biosciences*, *198*(2), 119–131.

Cai, L. M., & Li, X. Z. (2010). Global analysis of a vector-host epidemic model with nonlinear incidences. *Applied Mathematics and Computation*, *217*(7), 3531–3541.

Capasso, V., & Serio, G. (1978). A generalization of the kermack-mckendrick deterministic epidemic model. *Mathematical biosciences*, *42*(1-2), 43–61.

Das, K. P. (2016). A study of harvesting in a predator–prey model with disease in both populations. *Mathematical Methods in the Applied Sciences*, *39*(11), 2853–2870.

Dawed, M. Y., Tchepmo Djomegni, P. M., & Krogstad, H. E. (2020). Complex dynamics in a tritrophic food chain model with general functional response. *Natural Resource Modeling*, *33*(2), e12260.

Demir, M. (2019). Optimal control strategies in ecosystem-based fishery models.

Ghanbari, B. (2021). On the modeling of an eco-epidemiological model using a new fractional operator. *Results in physics*, *21*, 103799.

Gumel, A. B., & Moghadas, S. M. (2003). A qualitative study of a vaccination model with non-linear incidence. *Applied mathematics and computation*, *143*(2-3), 409–419.

Haldar, S., Khatua, A., Das, K., & Kar, T. K. (2021). Modeling and analysis of a predator–prey type eco-epidemic system with time delay. *Modeling Earth Systems and Environment*, *7*, 1753–1768.

Hale, J. K. (2009). *Ordinary differential equations*. Courier Corporation.

Haque, M., & Venturino, E. (2007). An ecoepidemiological model with disease in predator: The ratio-dependent case. *Mathematical methods in the Applied Sciences*, *30*(14), 1791–1809.

Holling, C. S. (1959). The components of predation as revealed by a study of small-mammal predation of the european pine sawfly1. *The canadian entomologist*, *91*(5), 293–320.

Hu, Z., Teng, Z., Zhang, T., Zhou, Q., & Chen, X. (2017). Globally asymptotically stable analysis in a discrete time eco-epidemiological system. *Chaos, Solitons & Fractals*, *99*, 20–31.

Hugo, A., & Simanjilo, E. (2019). Analysis of an eco-epidemiological model under optimal control measures for infected prey. *Applications and Applied Mathematics: An International Journal (AAM)*, *14*(1), 8.

Kooi, B. W., van Voorn, G. A., & pada Das, K. (2011). Stabilization and complex dynamics in a predator–prey model with predator suffering from an infectious disease. *Ecological Complexity*, *8*(1), 113–122.

Layek, G. C. (2015). *An introduction to dynamical systems and chaos* (Vol. 449). Springer.

Li, H., & Takeuchi, Y. (2011). Dynamics of the density dependent predator–prey system with beddington–deangelis functional response. *Journal of Mathematical Analysis and Applications*, *374*(2), 644–654.

Liu, W. M., Hethcote, H. W., & Levin, S. A. (1987). Dynamical behavior of epidemiological models with nonlinear incidence rates. *Journal of mathematical biology*, *25*, 359–380.

Lotka, A. J. (1925). *Elements of physical biology*. Williams; Wilkins.

Maiti, A. P., Jana, C., & Maiti, D. K. (2019). A delayed eco-epidemiological model with nonlinear incidence rate and crowley–martin functional response for infected prey and predator. *Nonlinear Dynamics*, *98*, 1137–1167.

Omar, F. M., Sohaly, M. A., & El-Metwally, H. (2024). Lyapunov functions and global stability analysis for epidemic model with n-infectious. *Indian Journal of Physics*, *98*(5), 1913–1922.

Panja, P. (2020). Prey–predator–scavenger model with monod–haldane type functional response. *Rendiconti del Circolo Matematico di Palermo Series 2*, *69*(3), 1205–1219.

Pirayesh, B., Pazirandeh, A., & Akbari, M. (2016). Local bifurcation analysis in nuclear reactor dynamics by sotomayor's theorem. *Annals of Nuclear Energy*, *94*, 716–731.

Ruan, S., & Wang, W. (2003). Dynamical behavior of an epidemic model with a nonlinear incidence rate. *Journal of differential equations*, *188*(1), 135–163.

Saifuddin, M., Biswas, S., Samanta, S., Sarkar, S., & Chattopadhyay, J. (2016). Complex dynamics of an eco-epidemiological model with different competition coefficients and weak allee in the predator. *Chaos, Solitons & Fractals*, *91*, 270–285.

Sieber, M., Malchow, H., & Hilker, F. M. (2014). Disease-induced modification of prey competition in eco-epidemiological models. *Ecological complexity*, *18*, 74–82.

Volterra, V. (1927). Fluctuations in the abundance of a species considered mathematically. *Nature*, *119*(2983), 12–13.

Wang, N., Zhao, M., Yu, H., Dai, C., Wang, B., & Wang, P. (2016). Bifurcation behavior analysis in a predator-prey model. *Discrete Dynamics in Nature and Society*, *2016*(1), 3565316.

Wayesa, N. N., Obsu, L. L., & Dawed, M. Y. (2024). Analysis of predator–prey model with inclusion of temperature variability in prey refugees. *Journal of Applied Mathematics*, *2024*(1), 5138320.

Wayesa, N. N., Obsu, L. L., & Dawed, M. Y. (2025). Predator–prey population dynamics with time delay and prey refuge effects. *Modeling Earth Systems and Environment*, *11*(2), 142.

Yu, X., Zhu, Z., Lai, L., & Chen, F. (2020). Stability and bifurcation analysis in a single-species stage structure system with michaelis–menten-type harvesting. *Advances in Difference Equations*, *2020*, 1–18.

Appendix A

let the Jacobian matrix the model(3) at the predator free equilibrium point $E^2(S^*, I^*, 0)$ denote by $J(E^2) = (\hat{A_{ij}})_{3\times3}$

$$J(E^2) = \begin{pmatrix} 1 - 2S^* - \kappa I^* - \dfrac{\gamma I^*}{1+\eta I^*} & -\kappa S^* - \dfrac{\gamma S^*}{(1+\eta I^*)^2} & -\theta_1\psi_S(S^*) \\ \dfrac{\gamma I^*}{1+\eta I^*} & \dfrac{\gamma S^*}{(1+\eta I^*)^2} - \zeta & -\theta_2\psi_I(I^*) \\ 0 & 0 & \psi_S(S^*) + \psi_I(I^*) - \xi \end{pmatrix}.$$

From the condition at which $J(E^2)$ has zero eigenvalue, that is, $\lambda_1 = \sigma_3 = \psi_S(S^*) + \psi_I(I^*) - \xi = 0$ the bifurcation value is

$$\hat{\xi} = \psi_S(S^*) + \psi_I(I^*).$$

Now we compute the Jacobian matrix $\hat{J}(E^2) = (\hat{A_{ij}})_{3\times3}$ at $\xi = \hat{\xi}$ which is same as above $J(E^2)$ except $\hat{A_{33}} = 0$. The eigenvectors of $\hat{J}(E^2, \hat{\xi})$ and $\hat{J}^T(E^2, \hat{\xi})$, corresponding to the zero eigenvalue are, respectively

$$V = \begin{pmatrix} \Psi_1\mathbf{e} \\ \mathbf{e} \\ \Psi_2\mathbf{e} \end{pmatrix} = \begin{pmatrix} V_1 \\ V_2 \\ V_3 \end{pmatrix} \text{ and } W = \begin{pmatrix} 0 \\ 0 \\ \mathbf{f} \end{pmatrix}$$

where, $\Psi_1 = \dfrac{\hat{A_{12}}\hat{A_{23}} - \hat{A_{22}}\hat{A_{13}}}{\hat{A_{21}}\hat{A_{13}} - \hat{A_{11}}\hat{A_{23}}}$, $\Psi_2 = \dfrac{\hat{A_{11}}\hat{A_{22}} - \hat{A_{12}}\hat{A_{21}}}{\hat{A_{21}}\hat{A_{13}} - \hat{A_{11}}\hat{A_{23}}}$, moreover $\mathbf{e}$ and $\mathbf{f}$ are nonzero real numbers. From our model system (3), we have:

$$F_\xi(X, \xi) = \begin{pmatrix} 0 \\ 0 \\ -P \end{pmatrix} \Longrightarrow F_\xi(E^2, \hat{\xi}) = \begin{pmatrix} 0 \\ 0 \\ 0 \end{pmatrix}$$

Thus, $W^T F_\xi(E^2, \hat{\xi}) = 0$. Applying Sotomayor's theorem (Pirayesh et al., 2016) for local bifurcation, the saddle node bifurcation does not occur near to the equilibrium point $E^2(S^*, I^*, 0)$. For Bogdanov– Takens bifurcation, there must be two equilibria : saddle and non-saddle. Therefore, BT bifurcation cannot appear here also.
We noted that the first condition $W^T F_\xi(E^2, \hat{\xi}) = 0$ of Sotomayor's theorem for the existence of transcritical bifurcation is satisfied. Now,

$$DF_\xi(E^2, \hat{\xi}) = \begin{pmatrix} 0 & 0 & 0 \\ 0 & 0 & 0 \\ 0 & 0 & -1 \end{pmatrix} \Longrightarrow DF_\xi(E^2, \hat{\xi})V = \begin{pmatrix} 0 & 0 & 0 \\ 0 & 0 & 0 \\ 0 & 0 & -1 \end{pmatrix} \begin{pmatrix} \Psi_1\mathbf{e} \\ \mathbf{e} \\ \Psi_2\mathbf{e} \end{pmatrix} = \begin{pmatrix} 0 \\ 0 \\ -\Psi_2\mathbf{e} \end{pmatrix}$$

So, we have $W^T[DF_\xi(E^2, \hat{\xi})V] = -\Psi_2\mathbf{ef} \neq 0$. Moreover,

$$D^2F(E^2, \hat{\xi})(V, V) = \begin{pmatrix} -2V_1^2 + \dfrac{2\gamma\eta S^*}{(1+\eta I^*)^3}V_2^2 - 2\left(\left(\kappa + \dfrac{\gamma}{(1+\eta I^*)^2}\right)V_1V_2 + \theta_1\psi_S'(S^*)V_3V_2\right) \\ \dfrac{-2\gamma\eta S^*}{(1+\eta I^*)^3}V_2^2 + 2\left(\dfrac{\gamma}{(1+\eta I^*)^2}V_1V_2 - \theta_2\psi_I'(I^*)V_2V_3\right) \\ 2V_3(\psi_S'(S^*)V_1 + \psi_I'(I^*)V_2) \end{pmatrix}$$

Thus, we have $W^T[D^2F(E^2, \hat{\xi})(V, V)] = 2V_3\mathbf{f}(\psi_S'(S^*)V_1 + \psi_I'(I^*)V_2) \neq 0$. Therefore, by Sotomayor's theorem, transcritical bifurcation occurs near to the predator-free stationary point $E^2(S^*, I^*, 0)$.

Appendix B

The Jacobian matrix of the system (3) at the infection free equilibrium point $E^3(S^*, 0, P^*)$ denote by $J(E^3) = (\overline{D_{ij}})_{3\times3}$ as

$$J(E^3) = \begin{pmatrix} 1 - 2S^* - \theta_1\psi_S'(S^*)P^* & -\kappa S^* - \gamma S^* & -\theta_1\psi_S(S^*) \\ 0 & \gamma S^* - \zeta - \theta_2\psi_I'(0)P^* & 0 \\ \psi_S'(S^*)P^* & \psi_I'(0)P^* & \psi_S(S^*) - \xi \end{pmatrix}.$$

Thus, $J(E^3)$ has zero eigenvalue, while, $\lambda_1 = \nabla_2 = \gamma_2 S^* - \zeta - \theta_2\psi_I'(0)P^* = 0$. and the model bifurcate when

$$\zeta^{[0]} = \frac{\theta_1\xi\gamma S^* - \theta_2\psi_I'(0)S^*(1 - S^*)}{\theta_1\xi}.$$

To perform the Jacobian matrix $J^{[0]}(E^3) = (D_{ij})_{3\times3}$ at $\zeta = \zeta^{[0]}$ which is same as above $J(E^3)$ except $D_{22} = 0$. The eigenvectors of $J^{[0]}(E^3, \zeta^{[0]})$ and $(J^{[0]}(E^3, \zeta^{[0]}))^T$, corresponding to the zero eigenvalue are, respectively

$$V = \begin{pmatrix} \Upsilon \\ \dfrac{D_{13}D_{31} - D_{11}D_{33}}{D_{12}D_{33} - D_{32}D_{13}}\Upsilon \\ \dfrac{D_{11}D_{32} - D_{12}D_{13}}{D_{12}D_{33} - D_{32}D_{13})}\Upsilon \end{pmatrix} = \begin{pmatrix} V_1 \\ V_2 \\ V_3 \end{pmatrix} \text{ and } W = \begin{pmatrix} 0 \\ \Gamma \\ 0 \end{pmatrix}$$

where,Υ and Γ are nonzero real numbers. From our model system (3), use derivative we get:

$$F_\zeta(X, \zeta) = \begin{pmatrix} 0 \\ -I \\ 0 \end{pmatrix} \Longrightarrow F_\zeta(E^3, \zeta^{[0]}) = \begin{pmatrix} 0 \\ 0 \\ 0 \end{pmatrix}$$

Thus, applying Sotomayor's theorem first condition $W^T F_\zeta(E^3, \zeta^{[0]}) = 0$. Hence, the dynamical system (3) saddle node bifurcation does not demonstrate at the disease free equilibrium point $E^3(S^*, 0, P^*)$.
Now we try to perform the other conditions of Sotomayor's theorem for the existence of transcritical bifurcation. Thus,

$$DF_\zeta(X, \zeta) = \begin{pmatrix} 0 & 0 & 0 \\ 0 & -1 & 0 \\ 0 & 0 & 0 \end{pmatrix}$$

$$\Longrightarrow DF_\zeta(E^3, \zeta^{[0]})V = \begin{pmatrix} 0 & 0 & 0 \\ 0 & -1 & 0 \\ 0 & 0 & 0 \end{pmatrix} \begin{pmatrix} \Upsilon \\ \dfrac{D_{13}D_{31} - D_{11}D_{33}}{D_{12}D_{33} - D_{32}D_{13}}\Upsilon \\ \dfrac{D_{11}D_{32} - D_{12}D_{13}}{D_{12}D_{33} - D_{32}D_{13})}\Upsilon \end{pmatrix} = \begin{pmatrix} 0 \\ \dfrac{D_{11}D_{33} - D_{13}D_{31}}{D_{12}D_{33} - D_{32}D_{13}}\Upsilon \\ 0 \end{pmatrix}$$

Hence, we arrived that $W^T[DF_\zeta(E^3, \zeta^{[0]})V] = \dfrac{D_{11}D_{33} - D_{13}D_{31}}{D_{12}D_{33} - D_{32}D_{13}}\Upsilon\Gamma \neq 0$. In addition,

$$D^2F(E^3, \zeta^{[0]})(V, V) = \begin{pmatrix} (-2 - \theta_1\psi_S''(S^*)P^*)V_1^2 + 2\gamma\eta S^* V_2^2 - 2\left((\kappa + \gamma 1)V_1V_2 + \theta_1\psi_S'(S^*)V_3V_2\right) \\ (-2\gamma\eta S^* - \theta_2\psi_I''(0)P^*)V_2^2 + 2(\gamma V_1V_2 - \theta_2\psi_I'(0)V_2V_3) \\ \psi_S''(S^*)P^*V_1^2 + \psi_I''(0)P^*V_2^2 + 2V_3(\psi_S'(S^*)V_1 + \psi_I'(0)V_2) \end{pmatrix}$$

Thus, we have

$$W^T[D^2F(E^3, \zeta^{[0]})(V, V)] = -(2\gamma\eta S^* + \theta_2\psi_I''(0)P^*)V_2^2\Upsilon + 2(\gamma V_1V_2\Upsilon - \theta_2\psi_I'(0)V_2V_3)\Upsilon \neq 0.$$

Therefore, according to Sotomayor's theorem (Pirayesh et al., 2016), our dynamical system (3) experience transcritical bifurcation at the disease-free fixed point $E^3(S^*, 0, P^*)$.